Calculation of Pion Valence Distribution from Hadronic Lattice Cross Sections

Raza Sabbir Sufian

in Collaboration with

J. Karpie, C. Egerer, D. Richards, J.W. Qiu, B. Chakraborty, R. Edwards, K. Orginos

Jefferson Lab
Thomas Jefferson National Accelerator Facility

Joe Karpie

Supervisor: K. Orginos

Major contribution in writing C++ code for pion and kaon

Involved in Pseudo-PDF calculation with A. Radyushkin and K. Orginos

Colin Egerer

Supervisor: D. Richards

Major contribution in writing C++ code for data handling

Involved in g_A calculation with D. Richards

Both supported by DOE's SCGSR Program

Why Pion Valence Distribution

★ Pion : lightest bound state and associated with dynamical chiral symmetry breaking

★ Pion valence distribution large-x behavior an unresolved problem

★ From pQCD and different models : $(1-x)^2$ or $(1-x)^1$?

★ C12-15-006 experiment at JLab to explore large-x behavior

(C. Weiss from Theory Center)

Why Pion Valence Distribution

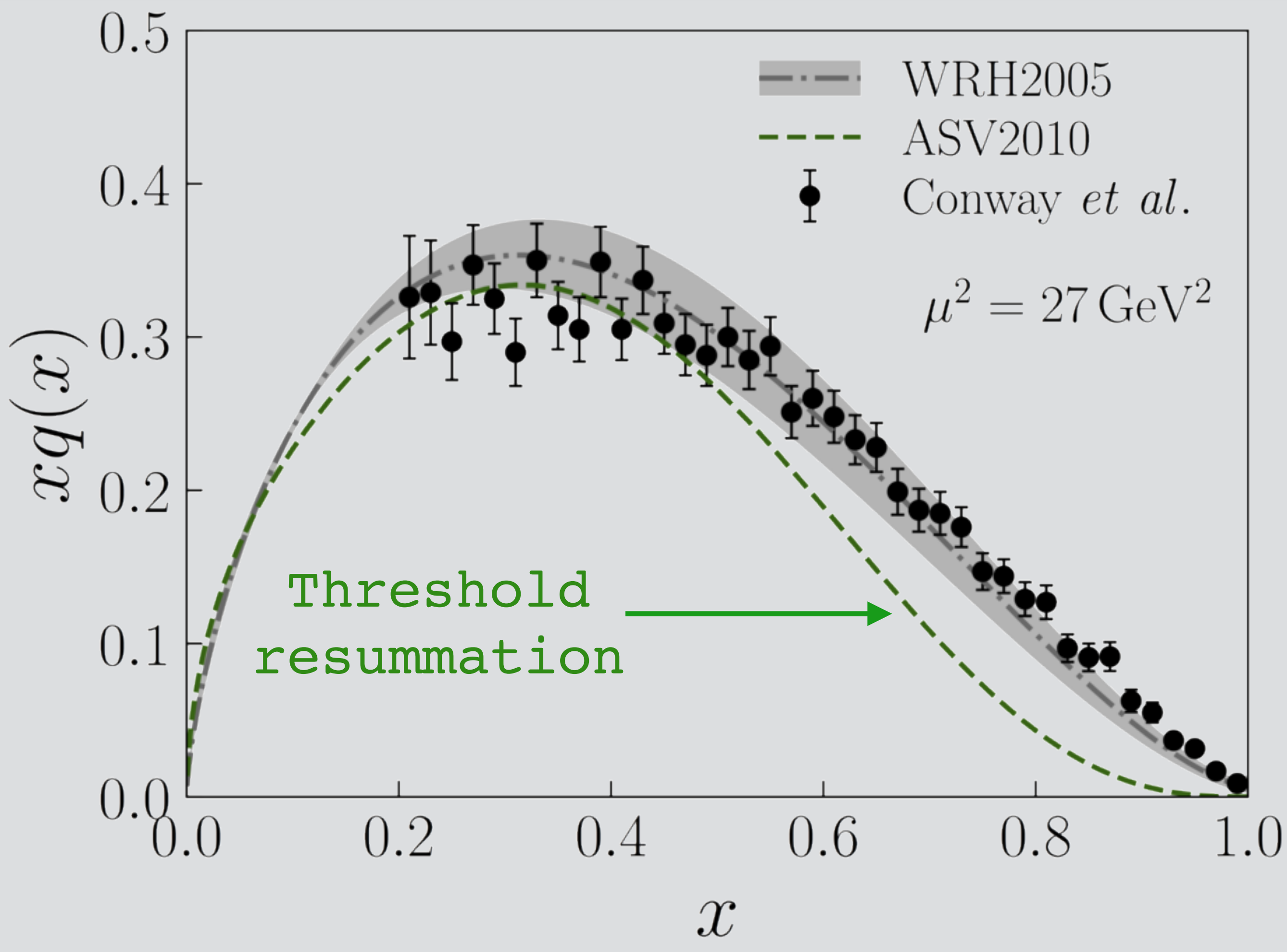

plot from Tianbo Liu

★ Large-x region: small configuration constrained by confinement dynamics

Lattice QCD can help understanding large-x behavior and test different models

Calculations of Parton Distributions on the Lattice

★ Quasi PDFs (X. Ji, PRL 2013)

$$\tilde{q}(x,\mu^2,P_z) \equiv \int \frac{d\xi_z}{4\pi} e^{-ixP_z\xi_z} \langle P|\bar{\psi}(\xi_z)\gamma_z \exp\left\{ -ig\int_0^{\xi_z} d\eta_z A_z(\eta_z)\right\}\psi(0)|P\rangle$$

Proposed Matching

$$\tilde{q}(x,\Lambda,P_z) = \int_{-1}^{1} \frac{dy}{|y|} Z\left(\frac{x}{y},\frac{\mu}{P_z},\frac{\Lambda}{P_z}\right)_{\mu^2=Q^2} q(y,Q^2) + \mathcal{O}\left(\frac{\Lambda^2_{QCD}}{P_z^2},\frac{M^2}{P_z^2}\right)$$

Power-law UV divergence from Wilson line in the non-local operator

★ Pseudo-PDFs (A. Radyushkin, PLB 2017)

$$M(\xi,P_Z) \to \mathcal{M}(\omega,\xi^2) \quad \text{Lorentz invariant Ioffe time } \omega = \xi\cdot P$$

$$\mathcal{P}(x,\xi^2) \equiv \int \frac{d\omega}{2\pi} e^{-ix\omega} \mathcal{M}(\omega,\xi^2)$$

Feature of canceling UV divergence from Wilson line

Lattice Implementation : 1. Orginos et. al (PRD 2017)

2. Gluon quasi-PDF (LP^3, 2018)

Calculations of Parton Distributions on the Lattice

- ★ Hadronic tensor (K. F. Liu, PRL 1994, PRD 200)
- ★ Position-space correlators (V. M. Braun & D. Müller, EPJ 2008)
- ★ Inversion Method (A. Chambers, et al PRL 2017)
- ★ Quasi PDFs (X. Ji, PRL 2013)
- ★ Pseudo-PDFs (A. Radyushkin, PLB 2017)

Extensive efforts and significant achievements in recent years

★ **Hadronic Lattice Cross Sections (LCSs)**
(Y. Q. Ma, J.-W. Qiu, PRL 2018)

What are Good Lattice "*Cross Sections*" (LCSs)

Single hadron matrix elements:

Ma & Qiu
PRL (2018)

1. Calculable using lattice QCD with Euclidean time

2. Well defined continuum limit ($a \to 0$), UV finite
i.e. no power law divergence from Wilson line in non-local operator

3. Share the same perturbative collinear divergences with PDFs

4. Factorizable to PDFs with IR-safe hard coefficients
with controllable power corrections

A good theory can identify its limitations

★ 4-point correlation function is numerically expensive

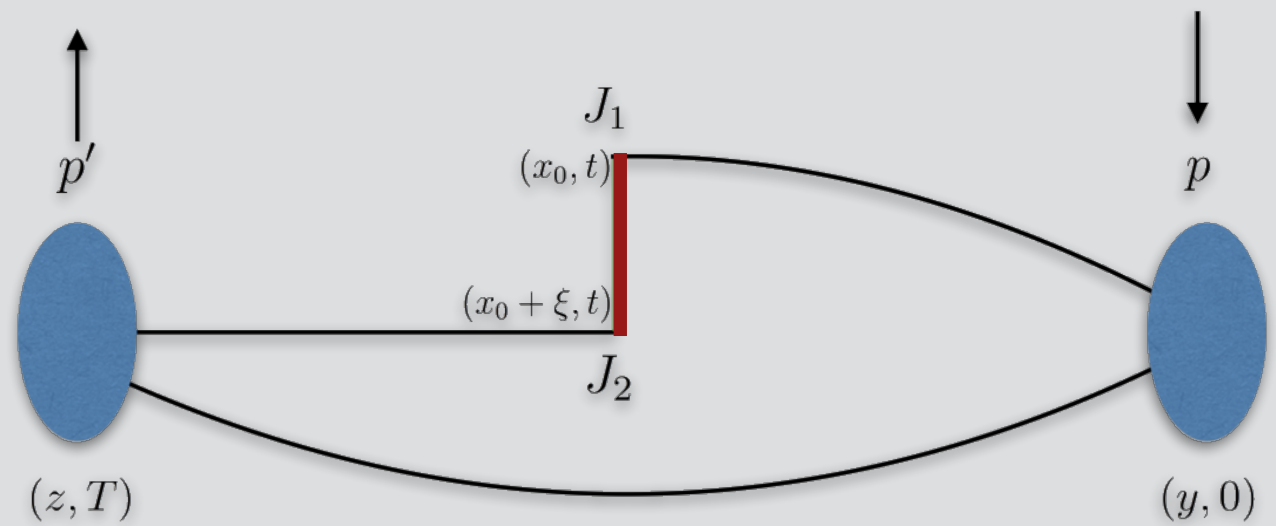

★ Equal time current insertion : sum over all energy modes can saturate phase space

Use heavy-light flavor changing current to suppress noise from spectator propagator in a systematic way

Simple and controllable approximations to problems

Good Lattice Cross Sections (LCSs)

★ **Hadron matrix elements:** $\sigma_n(\omega, \xi^2, P^2) = \langle P|T\{\mathcal{O}_n(\xi)\}|P\rangle$

$$\omega \equiv P \cdot \xi$$

★ **Current-current correlators**

$$\mathcal{O}_{j_1 j_2}(\xi) \equiv \xi^{d_{j_1}+d_{j_2}-2}\, Z_{j_1}^{-1}\, Z_{j_2}^{-1} j_1(\xi)\, j_2(0)$$

d_j : Dimension of the current

Z_j : Renormalization constant of the current

★ **Different choices of currents**

$$j_S(\xi) = \xi^2 Z_S^{-1}[\overline{\psi}_q \psi_q](\xi), \qquad j_V(\xi) = \xi Z_V^{-1}[\overline{\psi}_q \gamma \cdot \xi \psi_q](\xi),$$

$$j_{V'}(\xi) = \xi Z_{V'}^{-1}[\overline{\psi}_q \gamma \cdot \xi \psi_{q'}](\xi), \qquad j_G(\xi) = \xi^3 Z_G^{-1}[-\frac{1}{4} F^c_{\mu\nu} F^c_{\mu\nu}](\xi)\, , \ldots$$

flavor changing current

gluon distribution

Parton Distribution Functions (PDFs) & Factorization

$$\sigma^{DIS}(x, Q^2, \sqrt{s}) = \sum_{\alpha=q,\bar{q},g} C_\alpha\left(x, \frac{Q^2}{\mu^2}, \sqrt{s}\right) \otimes f_\alpha(x, \mu^2) + \text{Power Corrections}$$

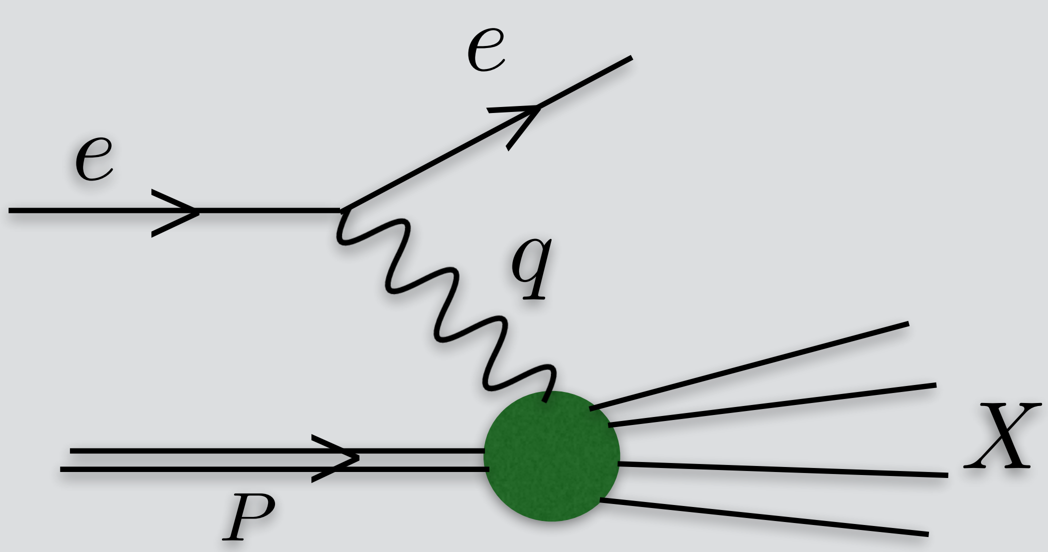

DIS

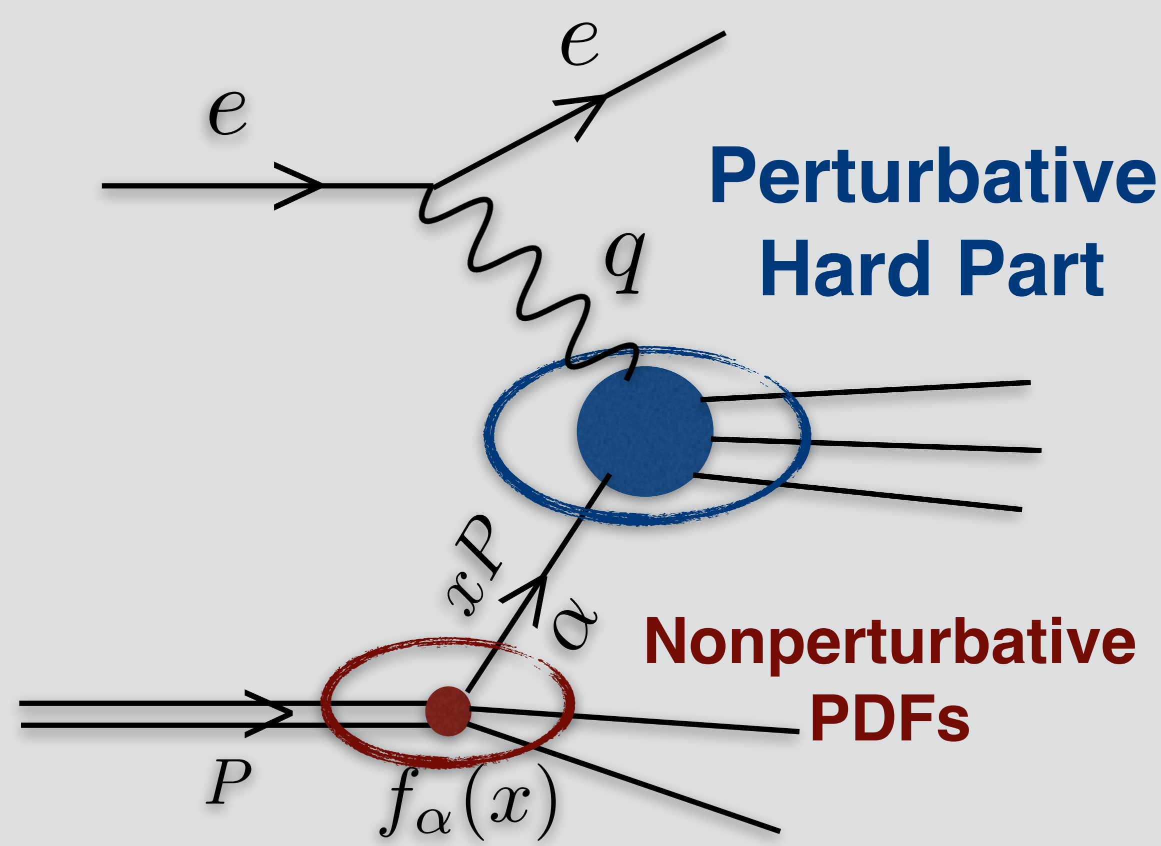

Parton Picture

Factorization scale μ describes which fluctuations should be included in the PDFs and which can be included in the hard scattering part

LCSs: Lattice Calculable + Renormalizable + Factorizable

$$\sigma_n(\omega,\xi^2,P^2) = \sum_a \int_{-1}^{1} \frac{dx}{x} f_a(x,\mu^2) \times K_n^a(x\omega,\xi^2,x^2P^2,\mu^2) + \mathcal{O}(\xi^2\Lambda_{QCD}^2)$$

Nonperturbative PDFs of flavor $a = q, g$

Perturbatively calculable hard hoefficients

$$f_{\bar{a}}(x,\mu^2) = -f_a(-x,\mu^2)$$

P and ξ → $P \rightarrow \sqrt{s}$ Collision energy

Collision Kinematics

$\xi \rightarrow \frac{1}{Q}$ Hard Probe

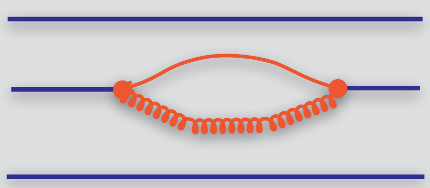

$\mathcal{O}_n$ → **Dynamical Features of LCSs**

LCSs : Factorization holds for any finite ω and $P^2\xi^2$ if ξ is short distance

Lattice Calculation

$$32^3 \times 96, \quad m_\pi \approx 430 \quad \text{MeV}$$
$$a \approx 0.127 \quad \text{fm}$$

Production Recently Finished

★ Projected calculations with

$$24^3 \times 64, \quad m_\pi \approx 430 \quad \text{MeV}$$
$$a \approx 0.127 \quad \text{fm}$$

Finite volume effect
Briceño, et al
PRD 2018

$$32^3 \times 64, \quad m_\pi \approx 280 \quad \text{MeV}$$
$$a \approx 0.09 \quad \text{fm}$$

Lattice spacing and pion mass effects

$$64^3 \times 128, \quad m_\pi \approx 170 \quad \text{MeV}$$
$$a \approx 0.09 \quad \text{fm}$$

Lattice Calculation Setup

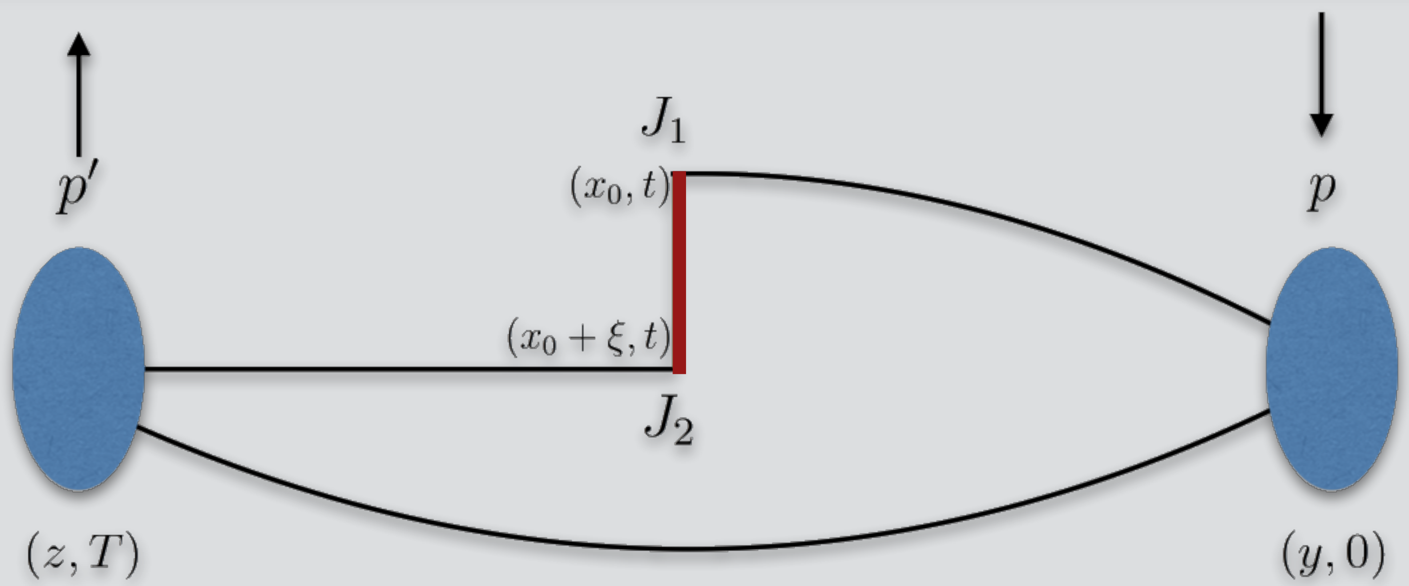

possible ξ
on/off axis

$$
\begin{aligned}
&\langle \Pi(-p')|\mathcal{O}_{J_1}(x_0)\mathcal{O}_{J_2}(\xi)|\Pi(-p')\rangle = \\
&\quad = \sum_{y,z} e^{i(p'.z-p.y)}\langle \bar{q}\,\Gamma_\Pi\, q(z,T)\,\bar{q}\,J_2\,q(x_0+\xi,t)\,\bar{q}\,J_1\,q(x_0,t)\,\bar{q}\,\Gamma_\Pi\,q(y,0)\rangle \\
&\quad = \sum_{y,z} e^{i(p'.z-p.y)}\mathrm{tr}[J_2\,D^{-1}(x_0+\xi,t;x_0,t)\,J_1\,D^{-1}(x_0,t;y,0)\,\Gamma_\Pi \\
&\qquad \times D^{-1}(y,0;z,T)\Gamma_\Pi\,D^{-1}(z,T;x_0+\xi,t)],
\end{aligned}
$$

★ Analysis shown here on isoClover with 490 Configurations

★ Lattice spacing ~ 0.127 fm, $m_\pi \approx 430$ MeV $(32^3 \times 96)$

Example Lattice Matrix Elements

★ About 10 different current-current correlations are being analyzed (R. Edwards for data handling)

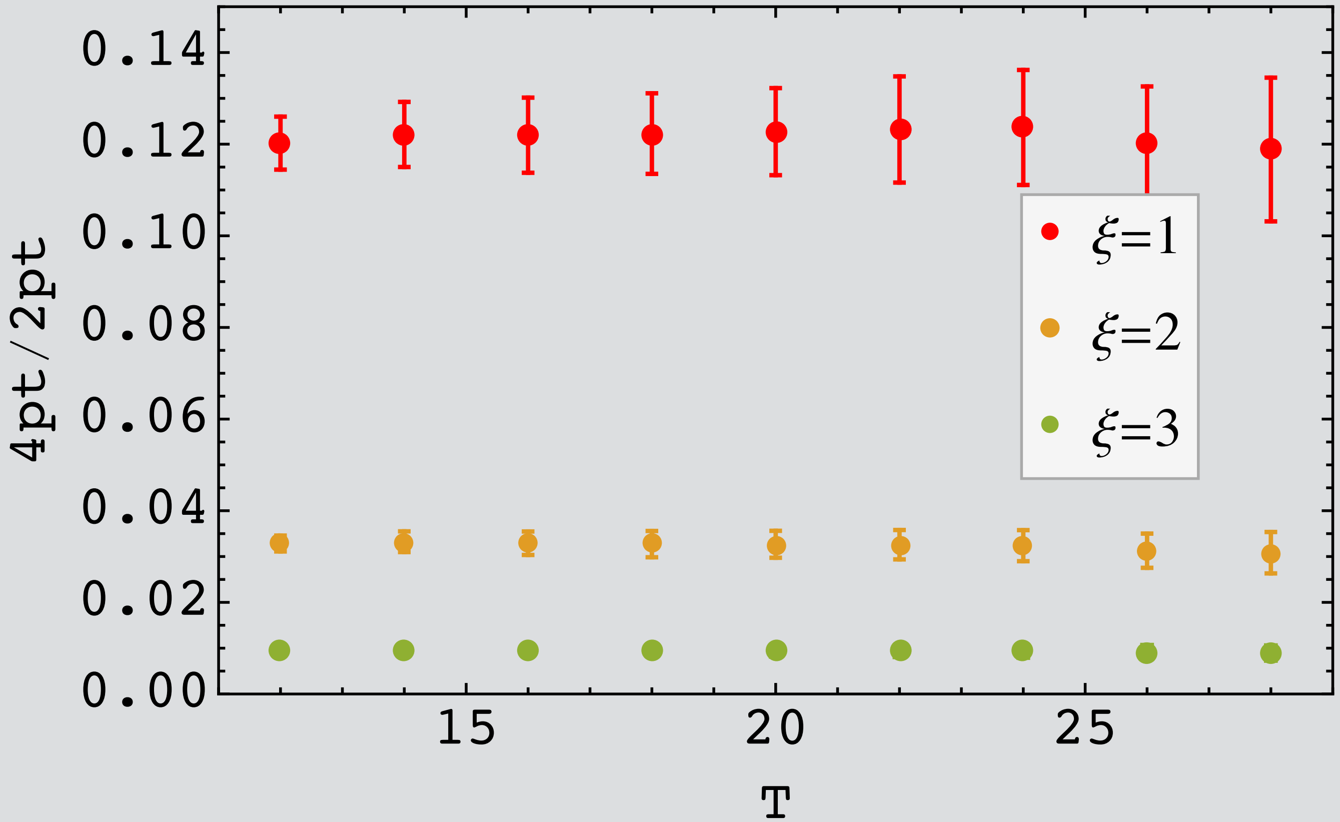

source-sink separation

V-A matrix element

Idea by **D. Richards** for reliable extraction of matrix elements

★ Momentum smearing used higher momentum

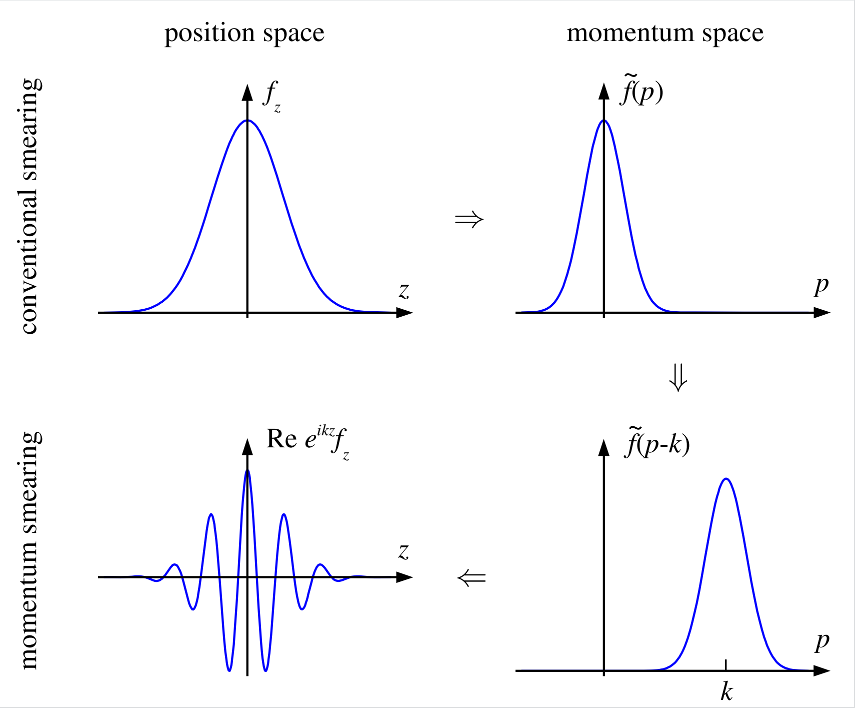

Bali, et al(PRD 2016)

Plots from Colin Egerer (50 configs)

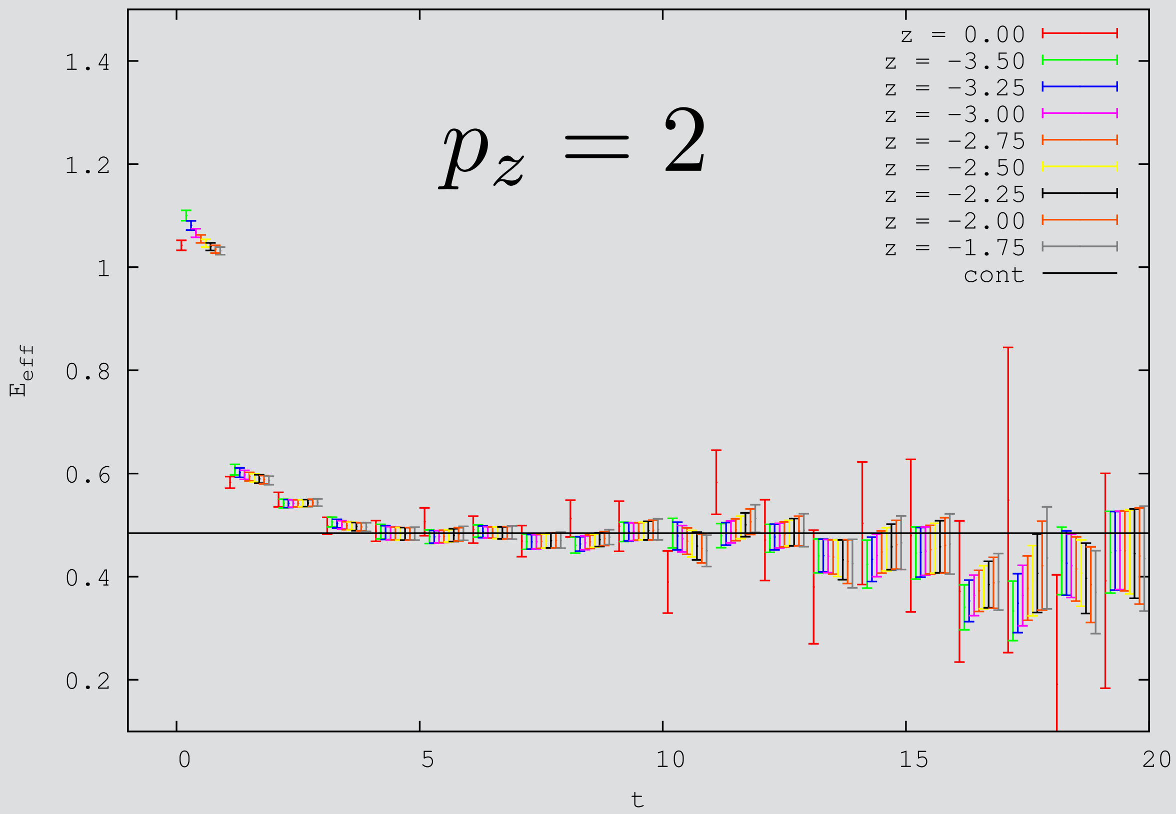

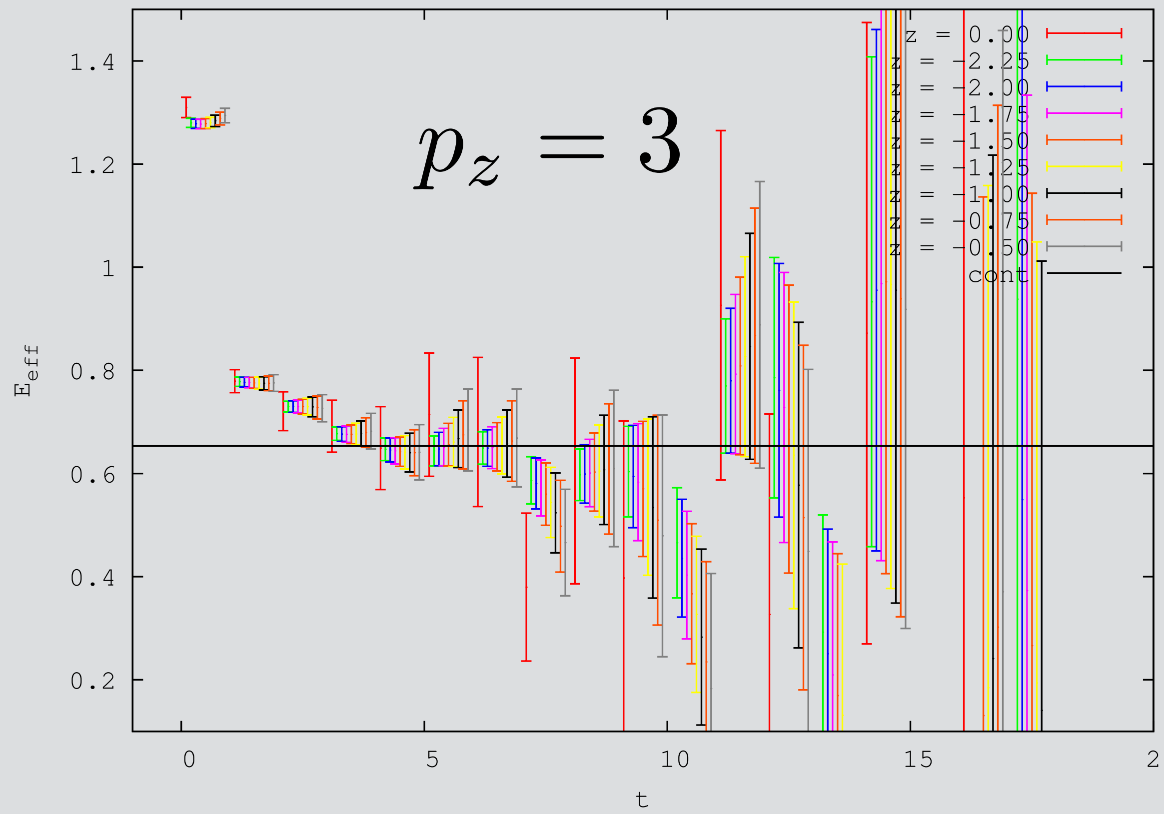

Preliminary Lattice Results

★ Only about 1/3 statistics of p=3,4,5 data analyzed and similar statistics from $\gamma_y - \gamma_y$ to be added

V-V current correlation

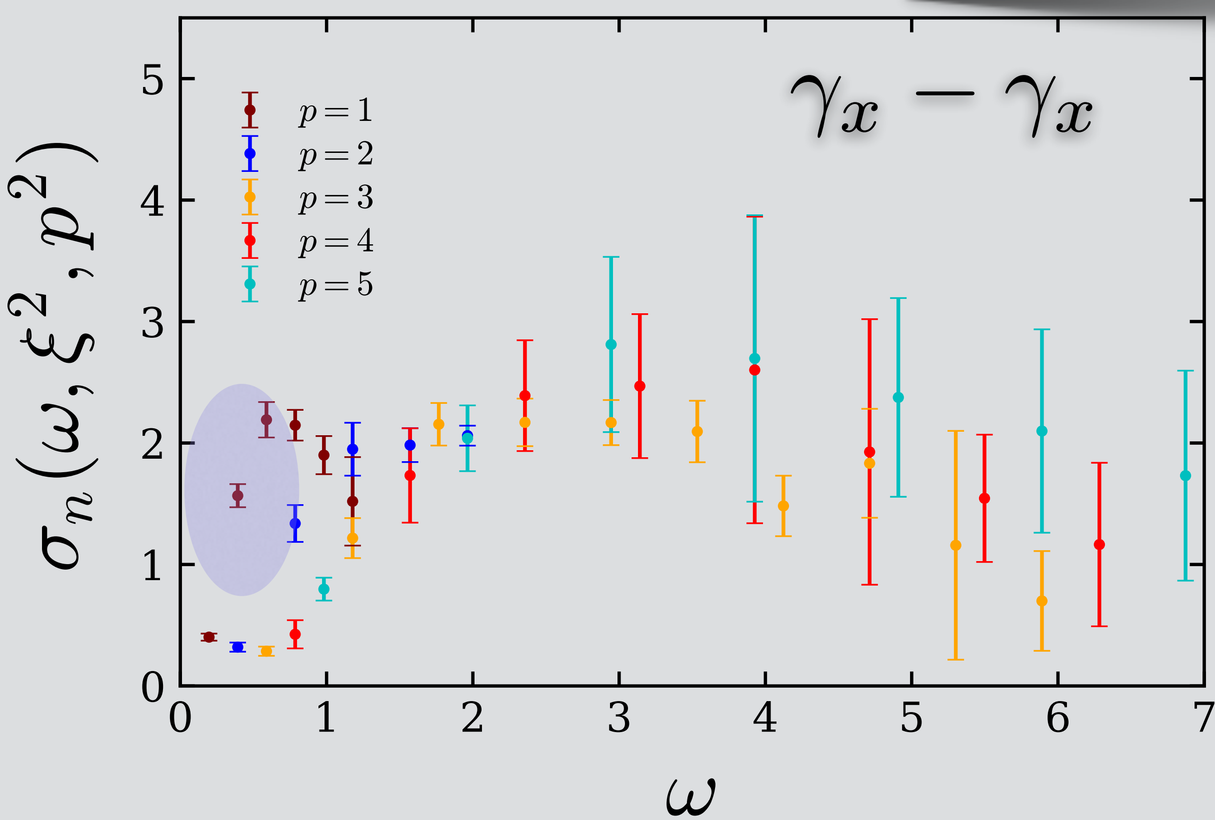

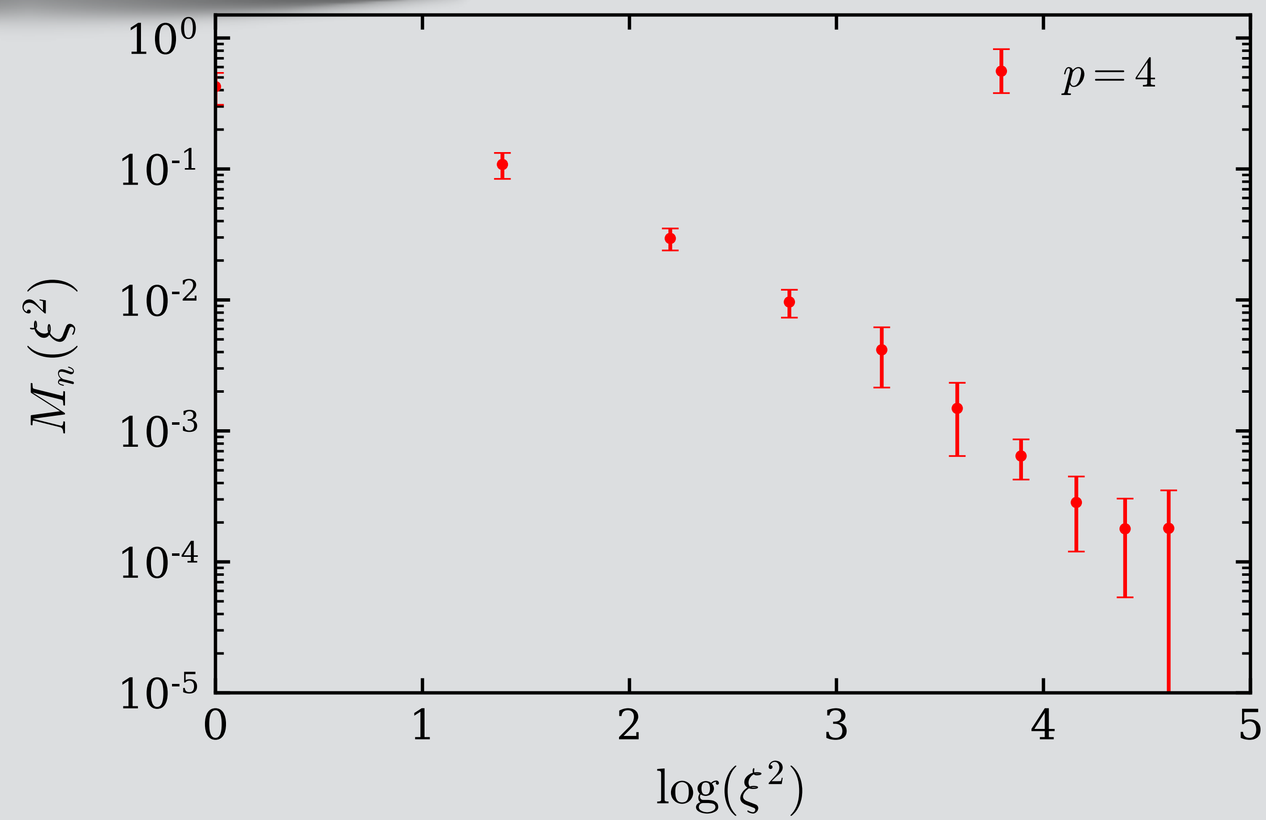

★ p=1 (0.3 GeV) data deviates

Does the calculated correlation matrix lead to consistent description of pion PDF ?

$$f(x) \approx Ax^{\alpha}(1-x)^{\beta}(1+\gamma\sqrt{x}+\delta x)$$

Preliminary Lattice Results

$$\sigma_n(\omega, \xi^2, P^2) = \sum_a \int_{-1}^{1} \frac{dx}{x} f_a(x, \mu^2) \times K_n^a(x\omega, \xi^2, x^2P^2, \mu^2) + \mathcal{O}(\xi^2\Lambda^2_{QCD})$$

calculate on lattice

extract PDF

PQCD

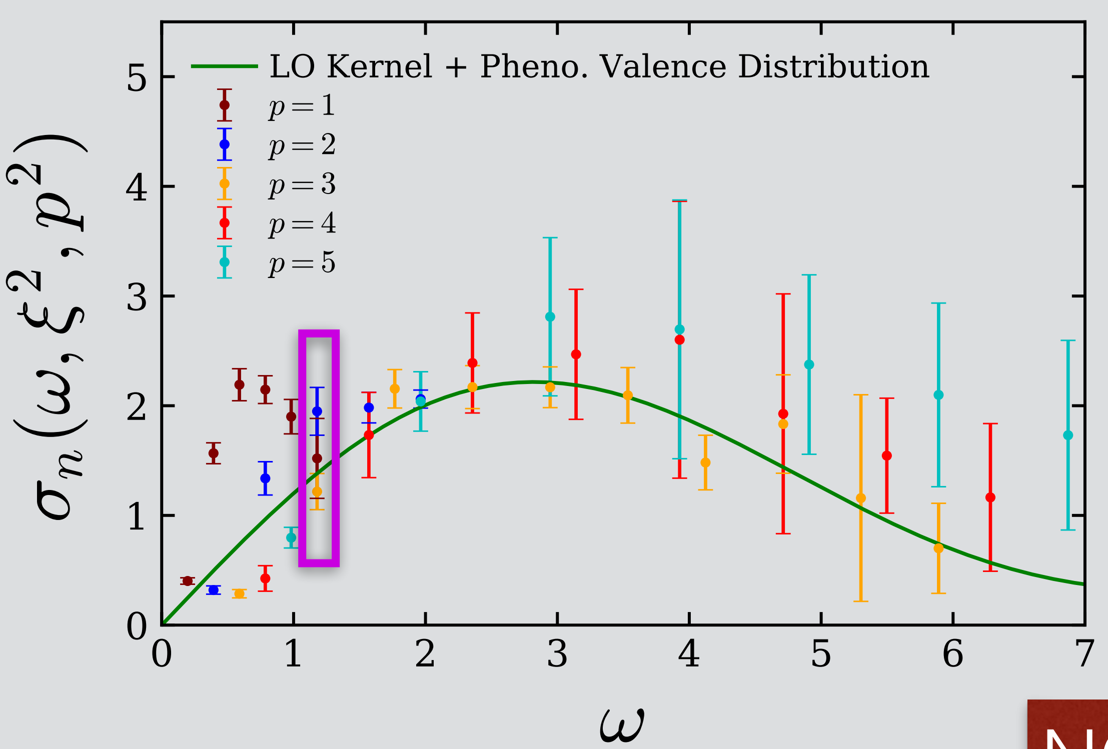

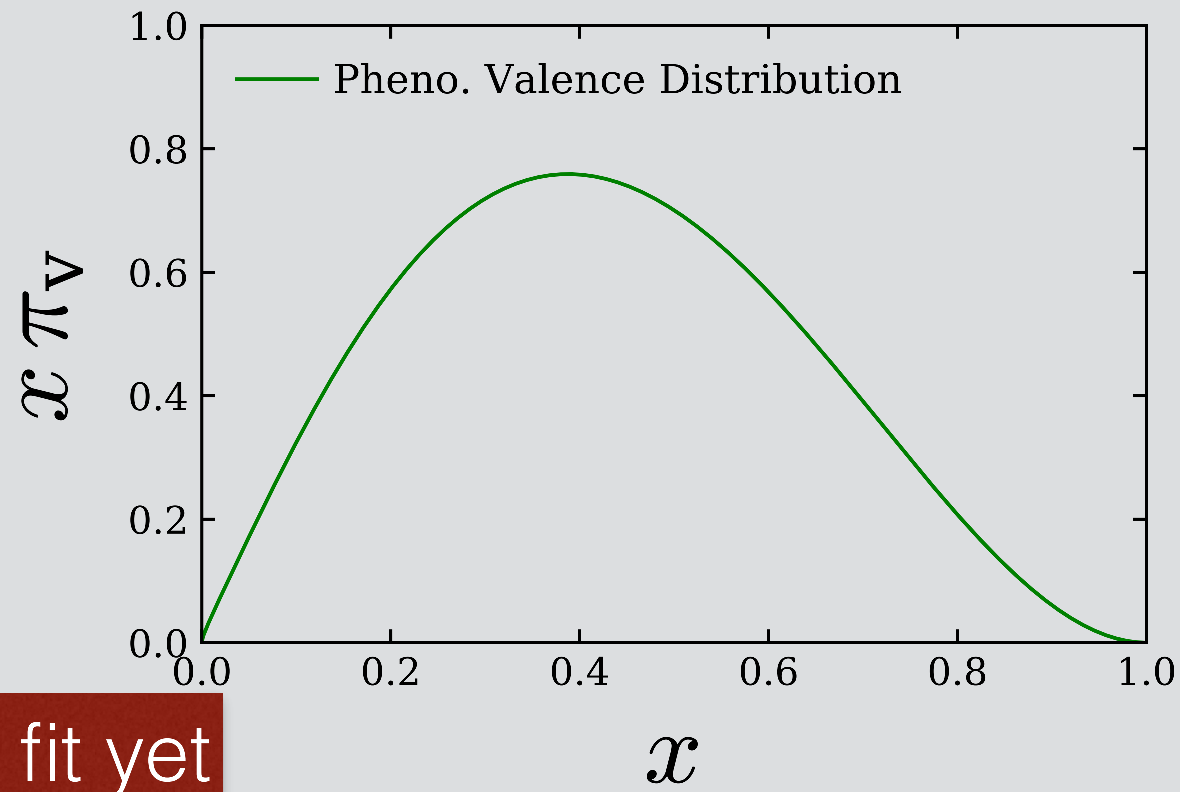

NOT a fit yet

★ A combined fit to many LCSs on an ensemble will lead to precise determination of PDFs

e.g. like global fits to data from different experiments !

With these encouraging results, we are very excited !!!

Collaboration between lattice QCD and perturbative QCD

LCSs can be a tool to test different model calculations

K_n^a at LO and NLO for different currents to be calculated

Extensions such as kaon, nucleon PDFs on their way....

Weak Neutral Current Axial Form Factors & (Anti)Neutrino Scattering

Raza Sabbir Sufian

in Collaboration with

David G. Richards & Keh-Fei Liu

Goals:

1. Determine WNC axial form factor &
2. Neutrino-nucleon scattering differential cross sections

Neutrino-Nucleon Neutral Current Elastic Scattering

$$\boxed{\begin{array}{ccc} \nu + p & \longrightarrow & \nu + p \\ \bar{\nu} + p & \longrightarrow & \bar{\nu} + p \end{array}}$$

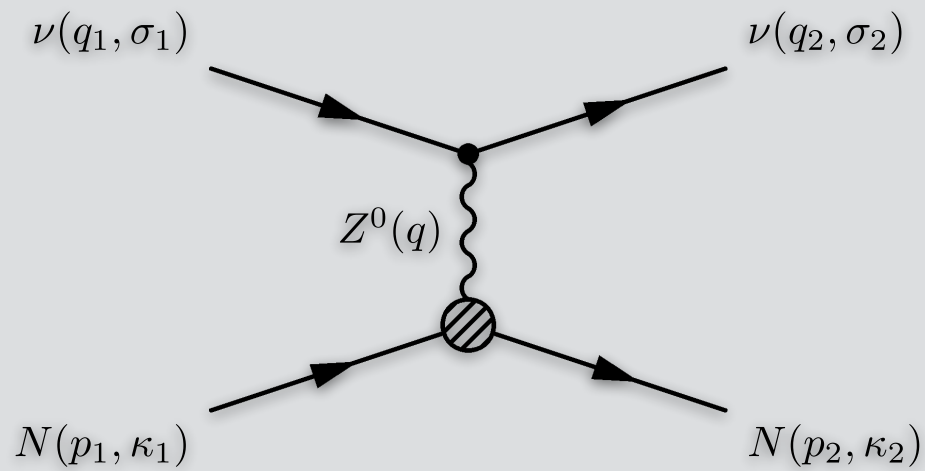

Matrix element in V-A structure of leptonic current

$$M = \frac{i}{2\sqrt{2}} G_F \underbrace{\bar{\nu}(q_2)\gamma_\mu(1-\gamma_5)\nu(q_1)}_{\text{leptonic current}} \underbrace{\langle N(p_2)| J_Z^\mu | N(p_1)\rangle}_{\text{hadronic current}} .$$

$$\boxed{\langle N(p_2)| \, J_Z^\mu \, |N(p_1)\rangle = \bar{u}(p_2)[F_1^Z(Q^2) + F_2^Z(Q^2)\frac{i\sigma^{\mu\nu}q_\nu}{2M_N} + F_A^Z(Q^2)\gamma^\mu\gamma_5]u(p_1)}$$

Eliminated from NCE scattering analysis by assuming different values of $\Delta s, \; M_A^{dipole}$ and dipole form of form factors

Weak Axial FF form parity-violating e-p scattering

$$
\begin{aligned}
A^p_{PV} = &-\frac{G_F Q^2}{4\sqrt{2}\pi\alpha}\frac{1}{[\epsilon(G^p_E)^2+\tau(G^p_M)^2]}\\
&\times\{(\epsilon(G^p_E)^2+\tau(G^p_M)^2)(1-4\sin^2\theta_W)(1+R^p_V)\\
&\quad-(\epsilon G^p_E G^n_E+\tau G^p_M G^n_M)(1+R^n_V)\\
&\quad-(\epsilon G^p_E G^s_E+\tau G^p_M G^s_M)(1+R^{(0)}_V)\\
&\quad-\epsilon'(1-4\sin^2\theta_W)G^p_M G^e_A\},
\end{aligned}
$$

with

$$
\tau=\frac{Q^2}{4M_p^2},\quad \epsilon=\left(1+2(1+\tau)\tan^2\frac{\theta}{2}\right)^{-1},
$$

$$
\epsilon'=\sqrt{\tau(1+\tau)(1-\epsilon^2)},
$$

$$
\mathcal{M}_\gamma=-\frac{4\pi\alpha}{Q^2}e_i l^\mu J^\gamma_\mu
$$

$$
\mathcal{M}_Z=\frac{G_F}{2\sqrt{2}}\left(g^i_V l^\mu+g^i_A l^{\mu 5}\right)\left(J^Z_\mu++J^Z_{\mu 5}\right)
$$

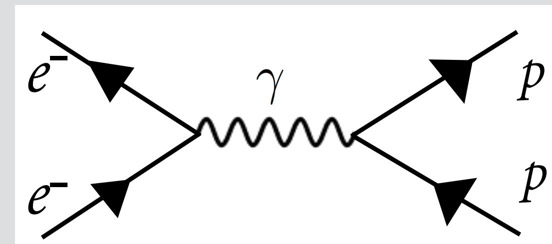

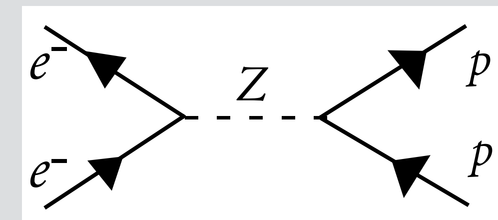

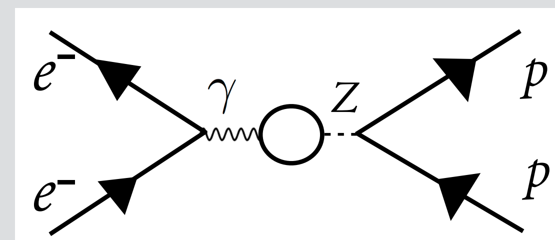

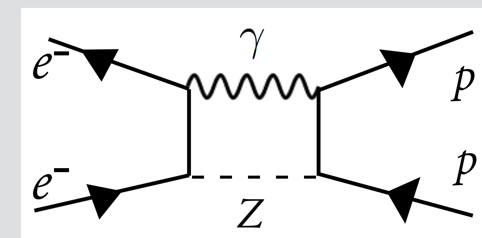

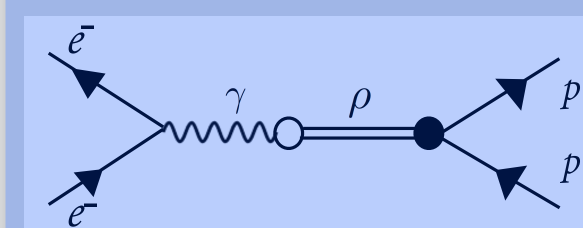

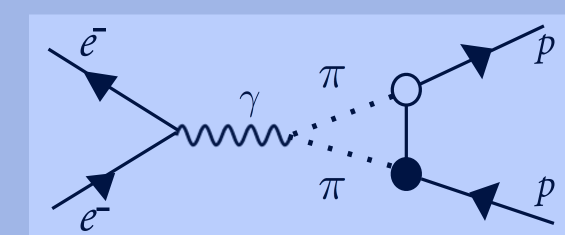

Qweak Collaboration, Nature 2018

$$
G_A^{eff}=-0.59(34)
$$

Many quark radiative corrections (unknown)

Goal of this work is to obtain the most precise determination of G_A^Z

(Anti)Neutrino-Nucleon Scattering Differential Cross Section

$$\boxed{\frac{d\sigma}{dQ^2} = \frac{G_F^2}{2\pi}\frac{Q^2}{E_\nu^2}(A \pm BW + CW^2)}$$

Garvey, PRC 1993

$$\boxed{W = 4(E_\nu/M_p - \tau)}$$

$$\boxed{A = \tfrac{1}{4}\{(G_A^Z)^2(1+\tau) - [(F_1^Z)^2 - \tau(F_2^Z)^2](1-\tau) + 4\tau F_1^Z F_2^Z\}}$$

$$\boxed{B = -\tfrac{1}{4}G_A^Z(F_1^Z + F_2^Z)}$$

$$\boxed{C = \frac{1}{64\tau}[(G_A^Z)^2 + (F_1^Z)^2 + \tau(F_2^Z)^2]}$$

Neutral Weak Dirac & Pauli FFs

Weak axial FF

Calculation of F_1^Z and F_2^Z

$$F_{1,2}^{Z,p} = \left(\frac{1}{2} - \sin^2\theta_W\right)(F_{1,2}^p(Q^2) - F_{1,2}^n(Q^2)) - \sin^2\theta_W(F_{1,2}^p + F_{1,2}^n) - \frac{F_{1,2}^s}{2}$$

Nucleon EMFF from Model Independent z-expansion

Ye, Arrington, Hill, Lee
PLB 2018

Two photon exchange correction included

Strange EMFF from Lattice QCD

RSS, et al. PRL (2017)
RSS, PRD 2018

Physical point
4 lattice spacings
3 volumes

Calculation of Neutral Weak EMFFs

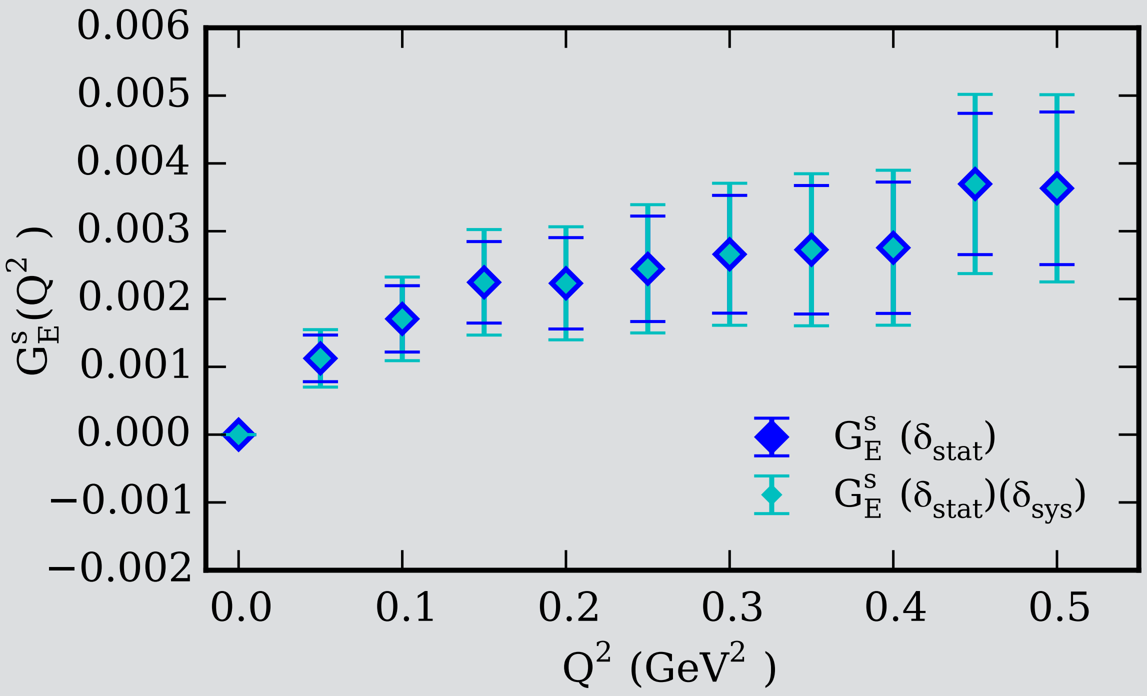

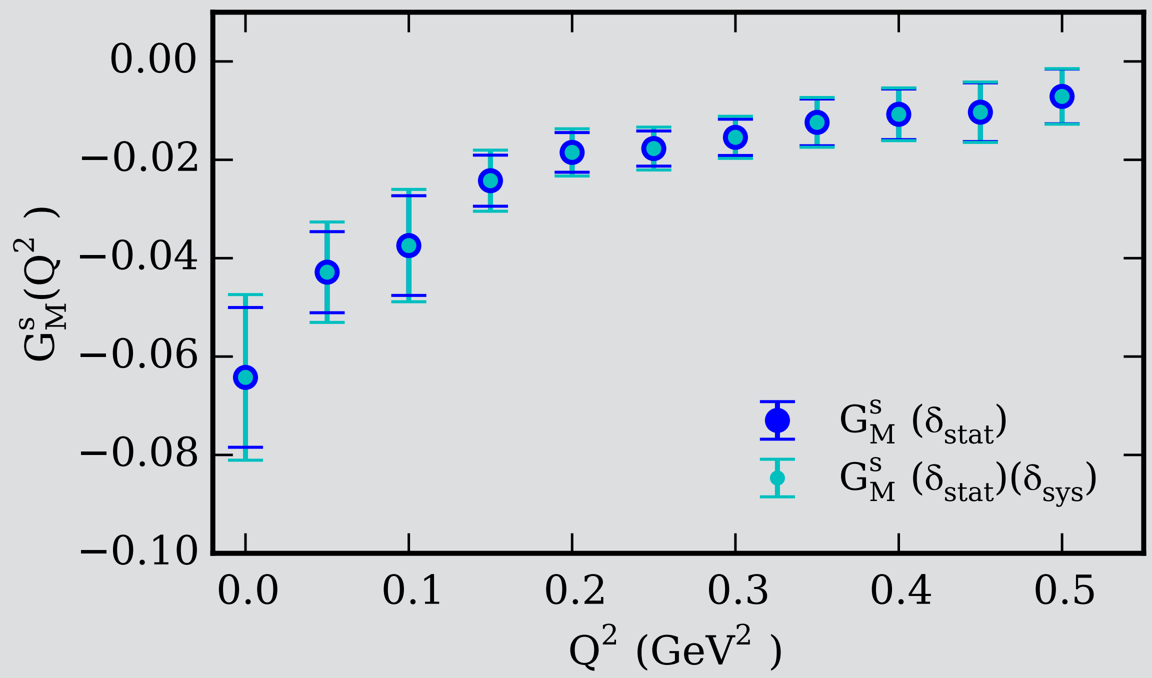

$$G_{E,M}^{Z,p(n)}(Q^2) = \frac{1}{4}\Big[(1-4\sin^2\theta_W)(1+R_V^{p(n)})G_{E,M}^{\gamma,p(n)}(Q^2) -(1+R_V^{n(p)})G_{E,M}^{\gamma,n(p)}(Q^2) - G_{E,M}^{s}(Q^2)\Big]$$

Radiative corrections for e-p scattering

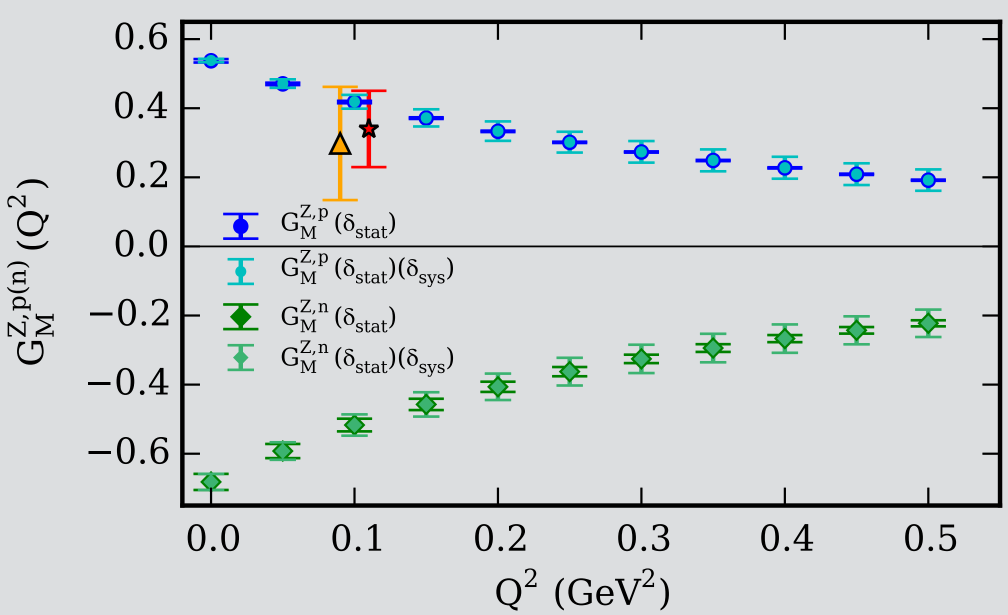

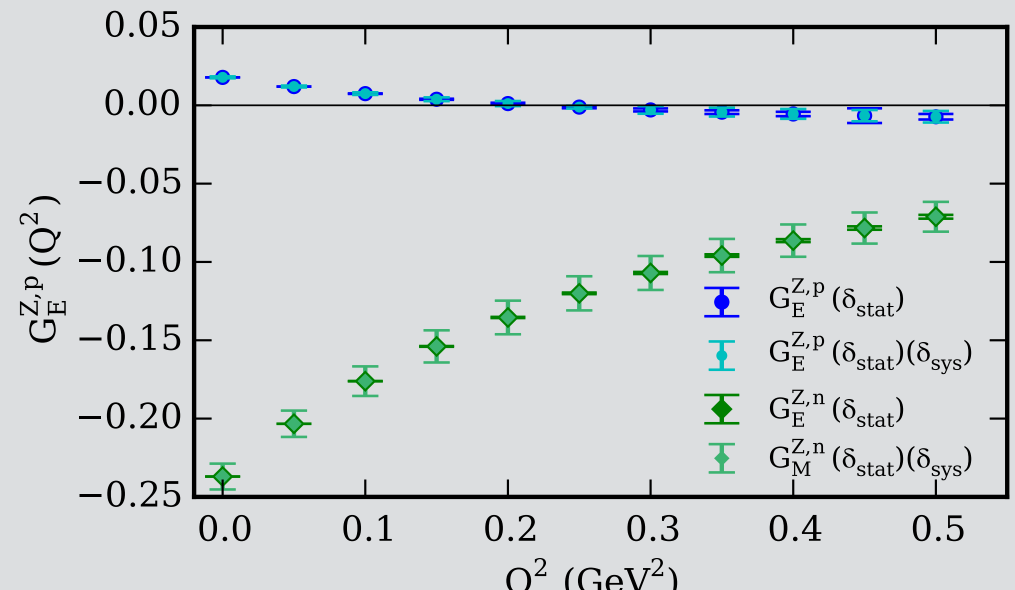

RSS, PRD 2017

Determination of Neutral Current Weak Axial FF

*Use MiniBooNE data ($0.27 < Q^2 < 0.70$ GeV^2)

Reason 1: Uncertainty in $G^s_{E,M}$ becomes very large and values consistent with zero

Reason 2: Nuclear effect can be large at low Q^2

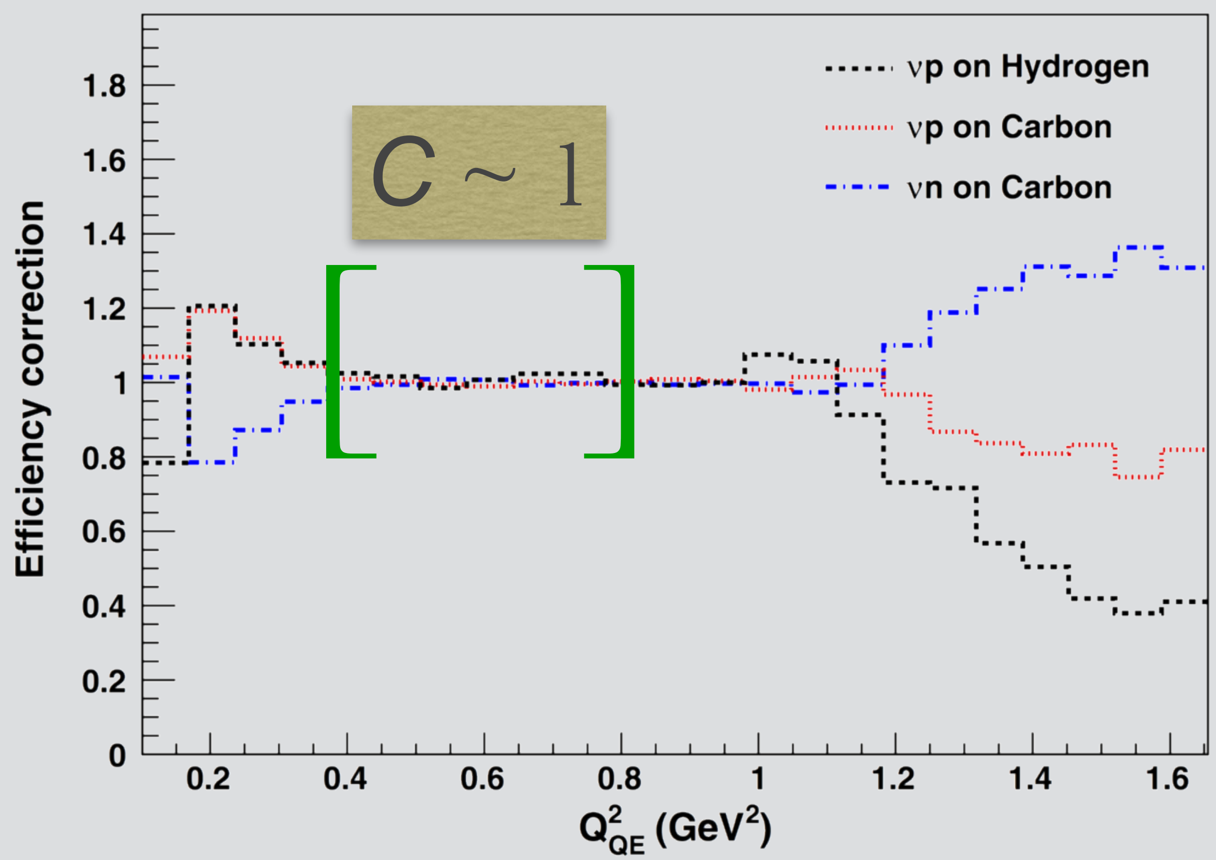

MiniBooNE used mineral oil CH_2 based Cherenkov detector

Determination of Neutral Current Weak Axial FF

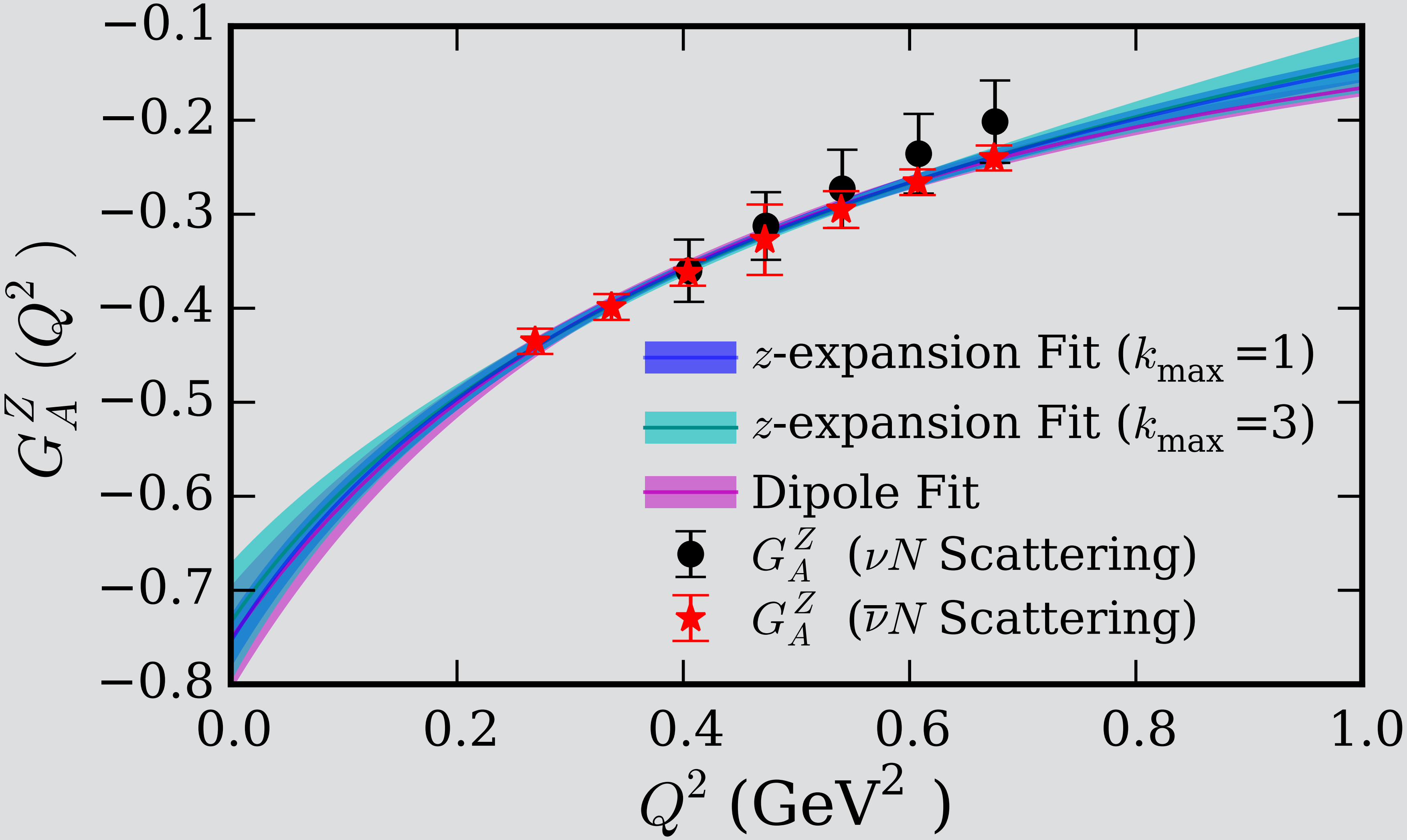

$$G_A^{Z,z-\exp}(Q^2) = \sum_{k=0}^{k_{\max}} a_k z^k, \quad z = \frac{\sqrt{t_{\text{cut}}+Q^2} - \sqrt{t_{\text{cut}}}}{\sqrt{t_{\text{cut}}+Q^2} + \sqrt{t_{\text{cut}}}}$$

z-exp fit	Fit parameters	$G_A^Z(0)$
2-terms	$a_1 = 1.378(92)$	-0.754(26)
3-terms	$a_1 = 1.260(359), a_2 = 0.200(623)$	-0.738(54)
4-terms	$a_1 = 1.248(367), a_2 = 0.127(973),$ $a_3 = 0.201(1.939)$	-0.734(63)
Dipole fit	$M_A^{\text{dip}} = 0.936(53)$ GeV	$-0.752(56)$

Impact of Lattice QCD Strange EMFF

Possibility: Since strange quark contribution is small

set $G^s_{E,M}$ =0 (??)

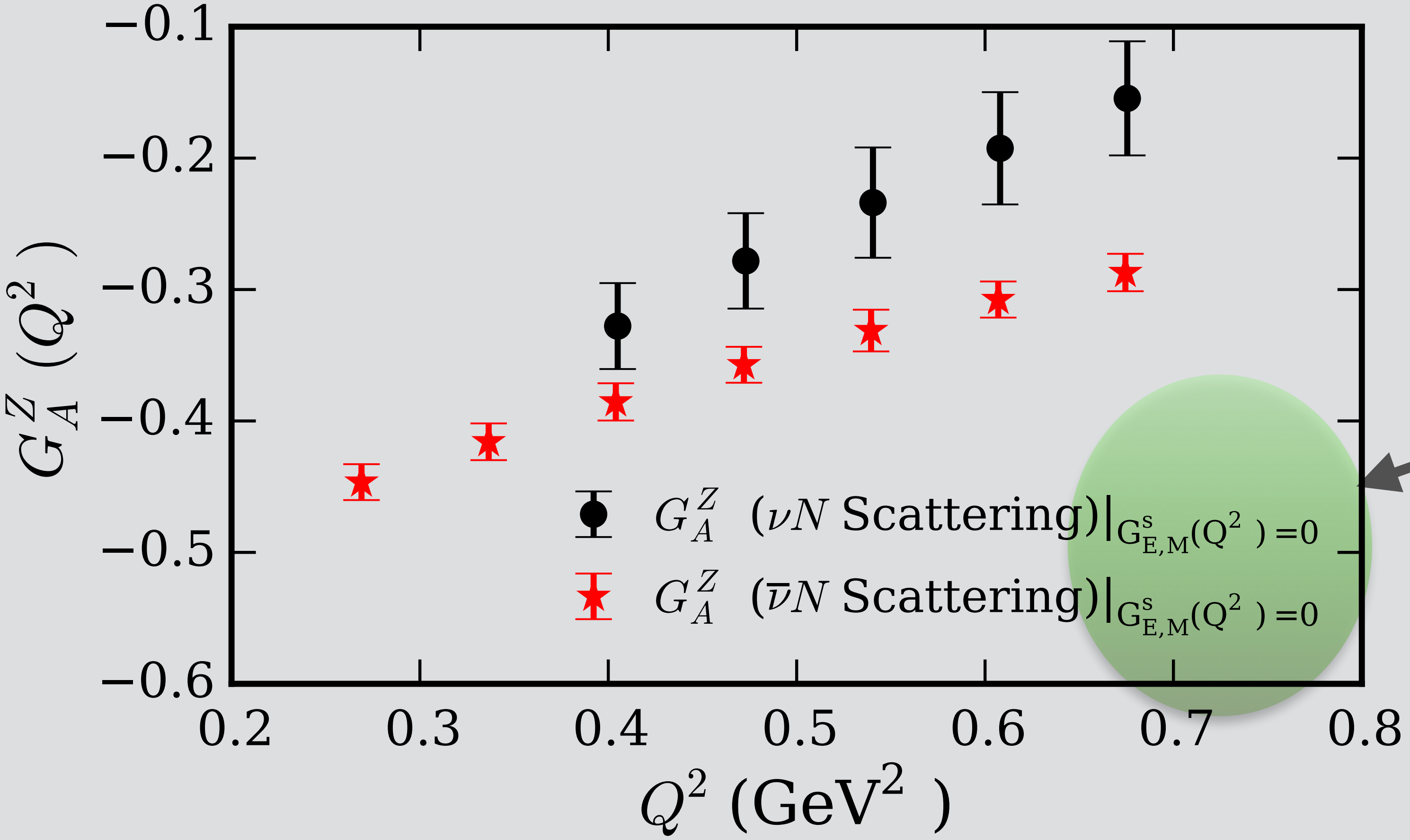

Discrepancy !!

$\cancel{G^s_{E,M}=0}$

Thanks to
[Rocco Schiavilla]

$$\frac{d\sigma}{dQ^2} = \frac{G_F^2}{2\pi}\frac{Q^2}{E_\nu^2}(A \pm BW + CW^2)$$

$$W = 4(E_\nu/M_p - \tau)$$

$$A = \tfrac{1}{4}\{(G_A^Z)^2(1+\tau) - [(F_1^Z)^2 - \tau(F_2^Z)^2](1-\tau) + 4\tau F_1^Z F_2^Z\}$$

$$B = -\tfrac{1}{4}G_A^Z(F_1^Z + F_2^Z)$$

$$C = \frac{1}{64\tau}[(G_A^Z)^2 + (F_1^Z)^2 + \tau(F_2^Z)^2]$$

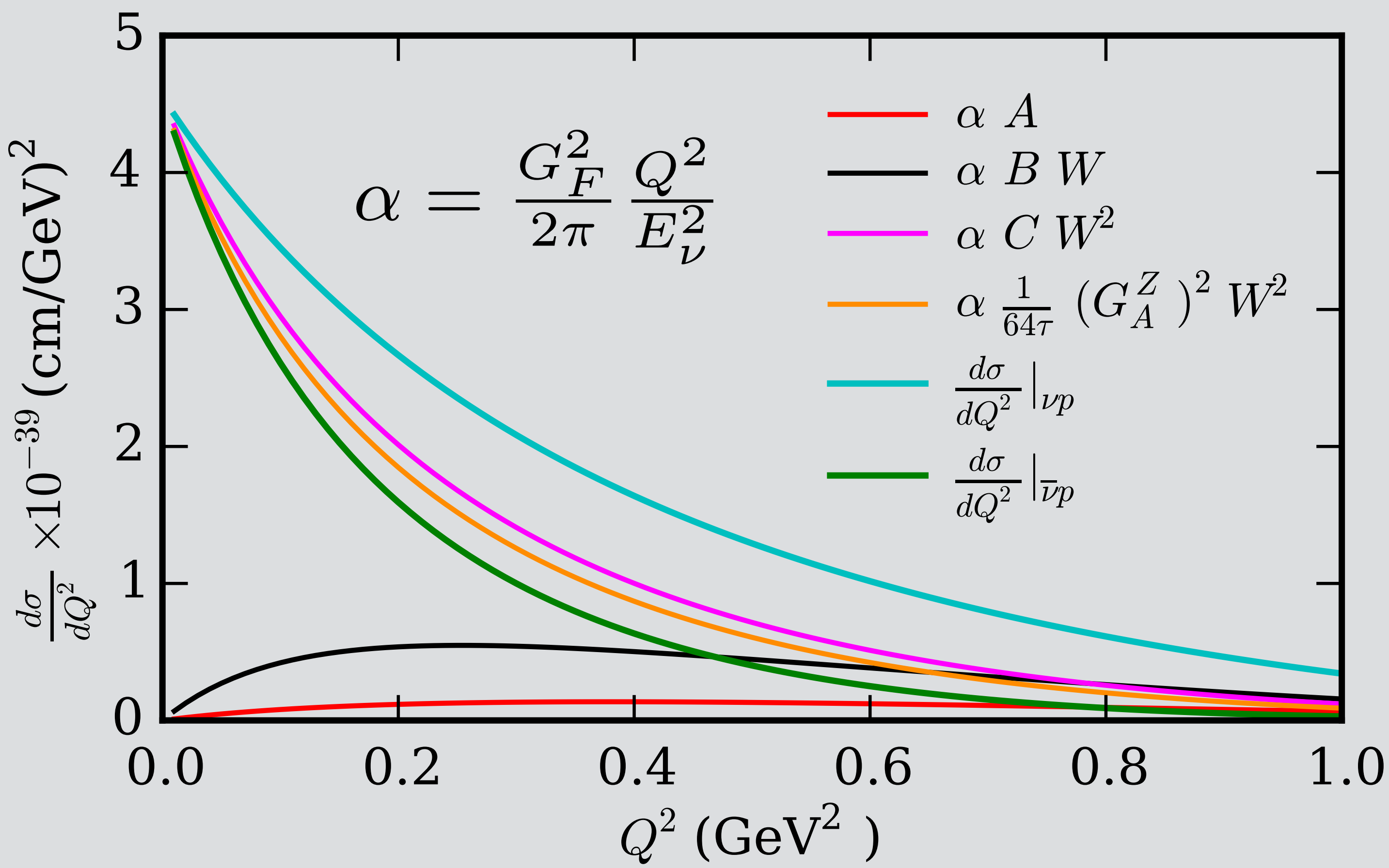

Dominant contribution from G_A^Z

Reconstruction of Differential Cross Sections

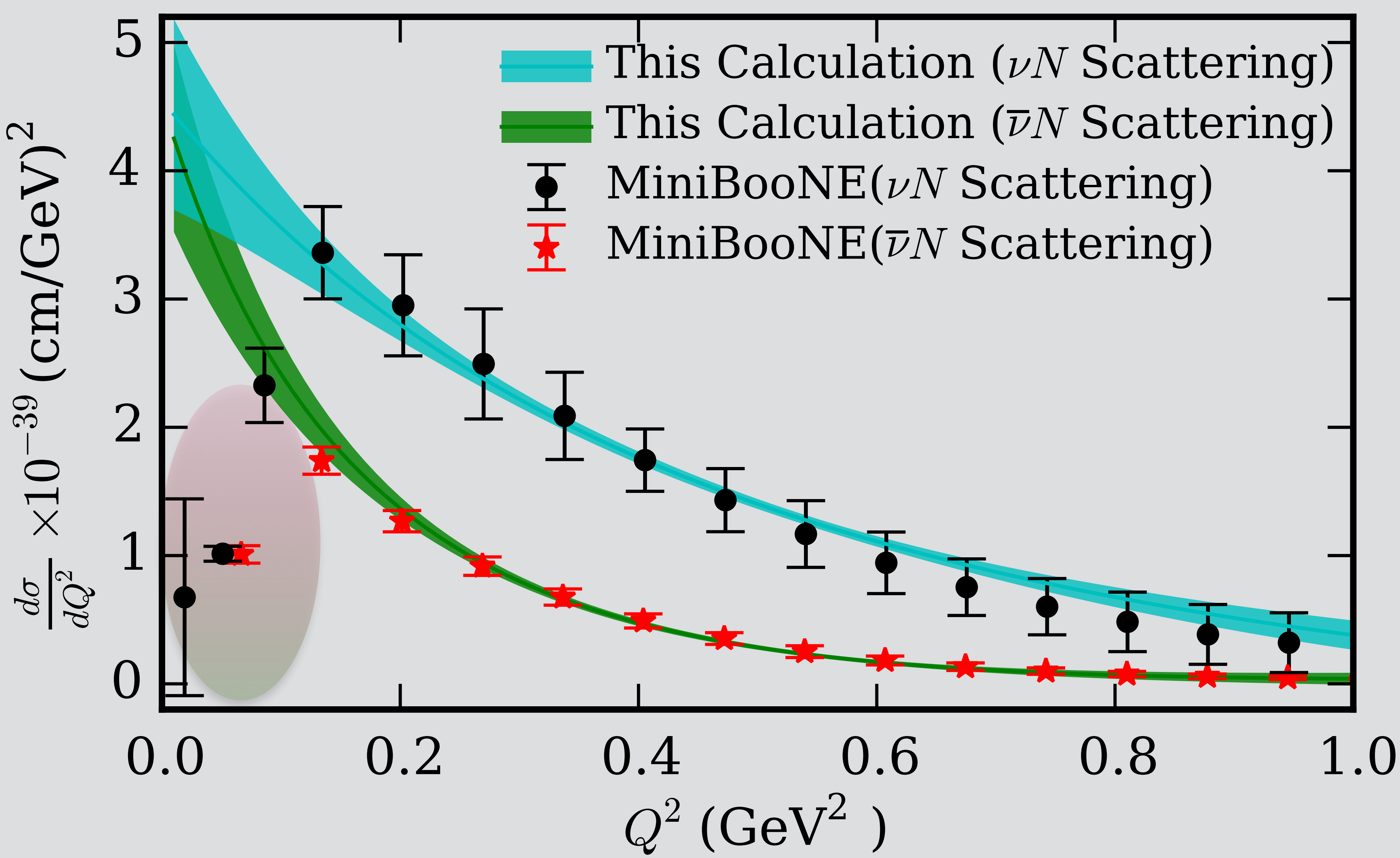

Nuclear effects
Pauli blocking included in simulation
Observed to have effect for $Q^2 < 0.15$ GeV^2

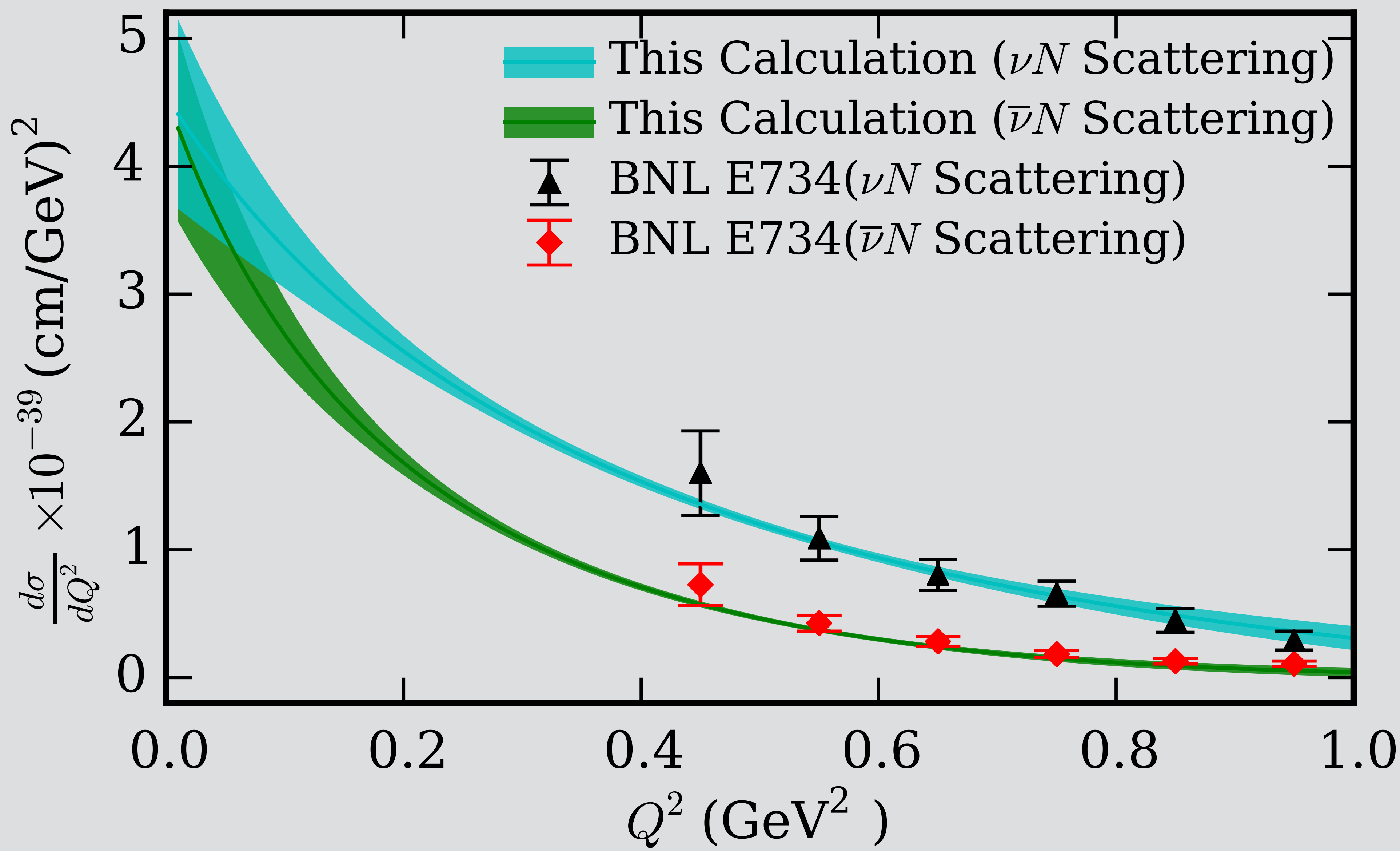

BNL E734 data
was NOT used in the analysis

Estimate of $G^s_A(0)$

This Calculation

$$\boxed{G_A^Z = \frac{1}{2}(-G_A^{CC} + G_A^s)}$$

$$\boxed{G_A^{CC}(0) = 1.2723(23)}$$

$$G_A^s(0) = -\ 0.196(127)(041)$$

MiniBooNE, PRD 82 (2010) $G_A^s(0) = 0.08(26)$

BNL E734, PRC 48 (1993)

$$G_A^s(0) = 0, -0.15(7), -0.13(09), -0.21(10)$$

(For various inputs of $G^s_{E,M}$)

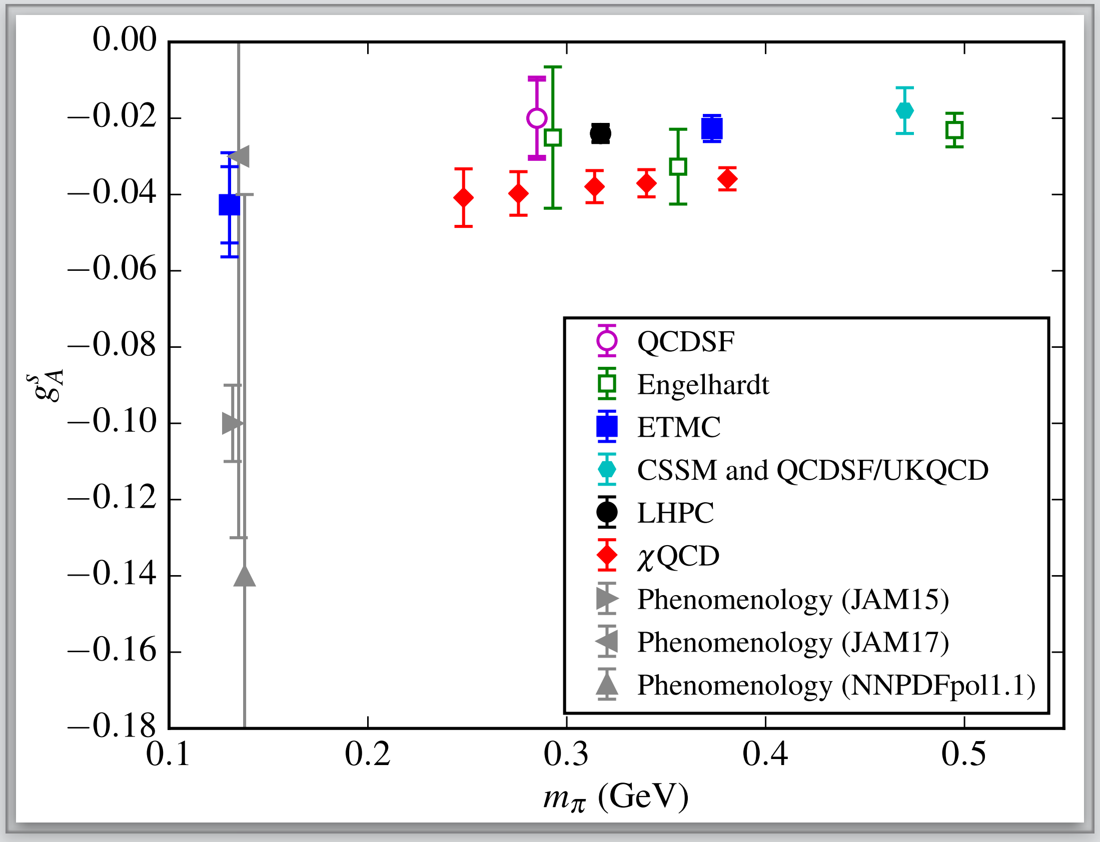

From Jeremy Green's Talk

Summary

- Precise estimate of NC weak axial form factor G^Z_A

- Strange quark contribution cannot be ignored

- Reconstruction of (anti)neutrino- nucleon diff. cross sections with correct prediction of G^Z_A and lattice input of $G^s_{E,M}$

- This calculation can be used to disentangle nuclear effects in neutrino-nucleus scattering experiments

#	CC / NC	Reaction
Cabibbo–allowed quasi–elastic scattering from nucleons		
1	CC	$\nu_\mu \mathrm{n} \to \mu^- \mathrm{p}$ ($\overline{\nu}_\mu \mathrm{p} \to \mu^+ \mathrm{n}$)
(Quasi–)elastic scattering from nucleons		
2	NC	$\nu_\mu \mathrm{n} \to \nu_\mu \mathrm{n}$ ($\overline{\nu}_\mu \mathrm{n} \to \overline{\nu}_\mu \mathrm{n}$) $\nu_\mu \mathrm{p} \to \nu_\mu \mathrm{p}$ ($\overline{\nu}_\mu \mathrm{p} \to \overline{\nu}_\mu \mathrm{p}$)
Resonant single pion production		
3	CC	$\nu_\mu \mathrm{p} \to \mu^- \mathrm{p} \pi^+$
4	CC	$\nu_\mu \mathrm{n} \to \mu^- \mathrm{p} \pi^0$
5	CC	$\nu_\mu \mathrm{n} \to \mu^- \mathrm{n} \pi^+$
6	NC	$\nu_\mu \mathrm{p} \to \nu_\mu \mathrm{p} \pi^0$
7	NC	$\nu_\mu \mathrm{p} \to \nu_\mu \mathrm{n} \pi^+$
8	NC	$\nu_\mu \mathrm{n} \to \nu_\mu \mathrm{n} \pi^0$
9	NC	$\nu_\mu \mathrm{n} \to \nu_\mu \mathrm{p} \pi^-$
10–16		Corresponding $\overline{\nu}_\mu$ processes
Multi–pion resonant processes		
17	CC	$\nu_\mu \mathrm{p} \to \mu^- \Delta^+ \pi^+$
18	CC	$\nu_\mu \mathrm{p} \to \mu^- \Delta^{++} \pi^0$
19	CC	$\nu_\mu \mathrm{n} \to \mu^- \Delta^+ \pi^0$
20	CC	$\nu_\mu \mathrm{n} \to \mu^- \Delta^0 \pi^+$
21	CC	$\nu_\mu \mathrm{n} \to \mu^- \Delta^{++} \pi^-$
22	NC	$\nu_\mu \mathrm{p} \to \nu_\mu \Delta^+ \pi^0$
23	NC	$\nu_\mu \mathrm{p} \to \nu_\mu \Delta^0 \pi^+$
24	NC	$\nu_\mu \mathrm{p} \to \nu_\mu \Delta^{++} \pi^-$
25	NC	$\nu_\mu \mathrm{n} \to \nu_\mu \Delta^+ \pi^-$
26	NC	$\nu_\mu \mathrm{n} \to \nu_\mu \Delta^0 \pi^0$
27	NC	$\nu_\mu \mathrm{n} \to \nu_\mu \Delta^- \pi^+$
28–38		Corresponding $\overline{\nu}_\mu$ processes
39	CC	$\nu_\mu \mathrm{p} \to \mu^- \mathrm{p} \rho^+(770)$
40	CC	$\nu_\mu \mathrm{n} \to \mu^- \mathrm{p} \rho^0(770)$
41	CC	$\nu_\mu \mathrm{n} \to \mu^- \mathrm{n} \rho^+(770)$
42	NC	$\nu_\mu \mathrm{p} \to \nu_\mu \mathrm{p} \rho^0(770)$
43	NC	$\nu_\mu \mathrm{p} \to \nu_\mu \mathrm{n} \rho^+(770)$
44	NC	$\nu_\mu \mathrm{n} \to \nu_\mu \mathrm{n} \rho^0(770)$
45	NC	$\nu_\mu \mathrm{n} \to \nu_\mu \mathrm{p} \rho^-(770)$
46–52		Corresponding $\overline{\nu}_\mu$ processes
53	CC	$\nu_\mu \mathrm{p} \to \mu^- \Sigma^+ \mathrm{K}^+$
54	CC	$\nu_\mu \mathrm{n} \to \mu^- \Sigma^0 \mathrm{K}^+$
55	CC	$\nu_\mu \mathrm{n} \to \mu^- \Sigma^+ \mathrm{K}^0$
56	NC	$\nu_\mu \mathrm{p} \to \nu_\mu \Sigma^0 \mathrm{K}^+$
57	NC	$\nu_\mu \mathrm{p} \to \nu_\mu \Sigma^+ \mathrm{K}^0$
58	NC	$\nu_\mu \mathrm{n} \to \nu_\mu \Sigma^0 \mathrm{K}^0$
59	NC	$\nu_\mu \mathrm{n} \to \nu_\mu \Sigma^- \mathrm{K}^+$
60–66		Corresponding $\overline{\nu}_\mu$ processes
67	CC	$\nu_\mu \mathrm{n} \to \mu^- \mathrm{p} \eta$
68	NC	$\nu_\mu \mathrm{p} \to \nu_\mu \mathrm{p} \eta$
69	NC	$\nu_\mu \mathrm{n} \to \nu_\mu \mathrm{n} \eta$
70–72		Corresponding $\overline{\nu}_\mu$ processes
73	CC	$\nu_\mu \mathrm{n} \to \mu^- \mathrm{K}^+ \Lambda$
74	NC	$\nu_\mu \mathrm{p} \to \nu_\mu \mathrm{K}^+ \Lambda$
75	NC	$\nu_\mu \mathrm{n} \to \nu_\mu \mathrm{K}^0 \Lambda$

Table 4.5: Processes available with NUANCE. The numbers in the leftmost column indicate the assigned reaction code in NUANCE.

#	CC / NC	Reaction
76–78		Corresponding $\overline{\nu}_\mu$ processes
79	CC	$\nu_\mu \mathrm{n} \to \mu^- \mathrm{p} \pi^+ \pi^-$
80	CC	$\nu_\mu \mathrm{n} \to \mu^- \mathrm{p} \pi^0 \pi^0$
81	NC	$\nu_\mu \mathrm{p} \to \nu_\mu \mathrm{p} \pi^+ \pi^-$
82	NC	$\nu_\mu \mathrm{p} \to \nu_\mu \mathrm{p} \pi^0 \pi^0$
83	NC	$\nu_\mu \mathrm{n} \to \nu_\mu \mathrm{n} \pi^+ \pi^-$
84	NC	$\nu_\mu \mathrm{n} \to \nu_\mu \mathrm{n} \pi^0 \pi^0$
85–90		Corresponding $\overline{\nu}_\mu$ processes
Deep Inelastic Scattering		
91	CC	$\nu_\mu \mathrm{N} \to \mu \mathrm{X}$
92	NC	$\nu_\mu \mathrm{N} \to \nu_\mu \mathrm{X}$
93–94		Unused
95	CC	Cabibbo–supp. QE hyperon production: $\overline{\nu}_\mu \mathrm{p} \to \mu^+ \Lambda$ $\overline{\nu}_\mu \mathrm{n} \to \mu^+ \Sigma^-$ $\overline{\nu}_\mu \mathrm{p} \to \mu^+ \Sigma^0$
Coherent / diffractive π production		
96	NC	$\nu_\mu \mathrm{A} \to \nu_\mu \mathrm{A} \pi^0$ $(\overline{\nu}_\mu \mathrm{A} \to \overline{\nu}_\mu \mathrm{A} \pi^0)$
97	CC	$\nu_\mu \mathrm{A} \to \mu^- \mathrm{A} \pi^+$ $(\overline{\nu}_\mu \mathrm{A} \to \mu^+ \mathrm{A} \pi^-)$
ν–e elastic scattering		
98	–	$\nu_\mu \mathrm{e} \to \nu_\mu \mathrm{e}$ $(\overline{\nu}_\mu \mathrm{e} \to \overline{\nu}_\mu \mathrm{e})$
ν–e inverse μ decay		
99	CC	$\nu_\mu \mathrm{e} \to \mu^- \nu_\mathrm{e}$

Table 4.5: Processes available with NUANCE. The numbers in the leftmost column indicate the assigned reaction code in NUANCE.(Continued from the previous page)

S.F. Pate, Phys. Rev. Lett. **92**, 082002 (2004)

TABLE II. Two solutions for the strange form factors at $Q^2 = 0.5\ \mathrm{GeV}^2$ produced from the E734 and HAPPEX data.

	Solution 1	Solution 2
G_E^s	0.02 ± 0.09	0.37 ± 0.04
G_M^s	0.00 ± 0.21	-0.87 ± 0.11
G_A^s	-0.09 ± 0.05	0.28 ± 0.10

$Q^2 = 0.5\ \mathrm{GeV}^2$

Pate, et al

EPJ Web Conf. 66 (2014) 06018

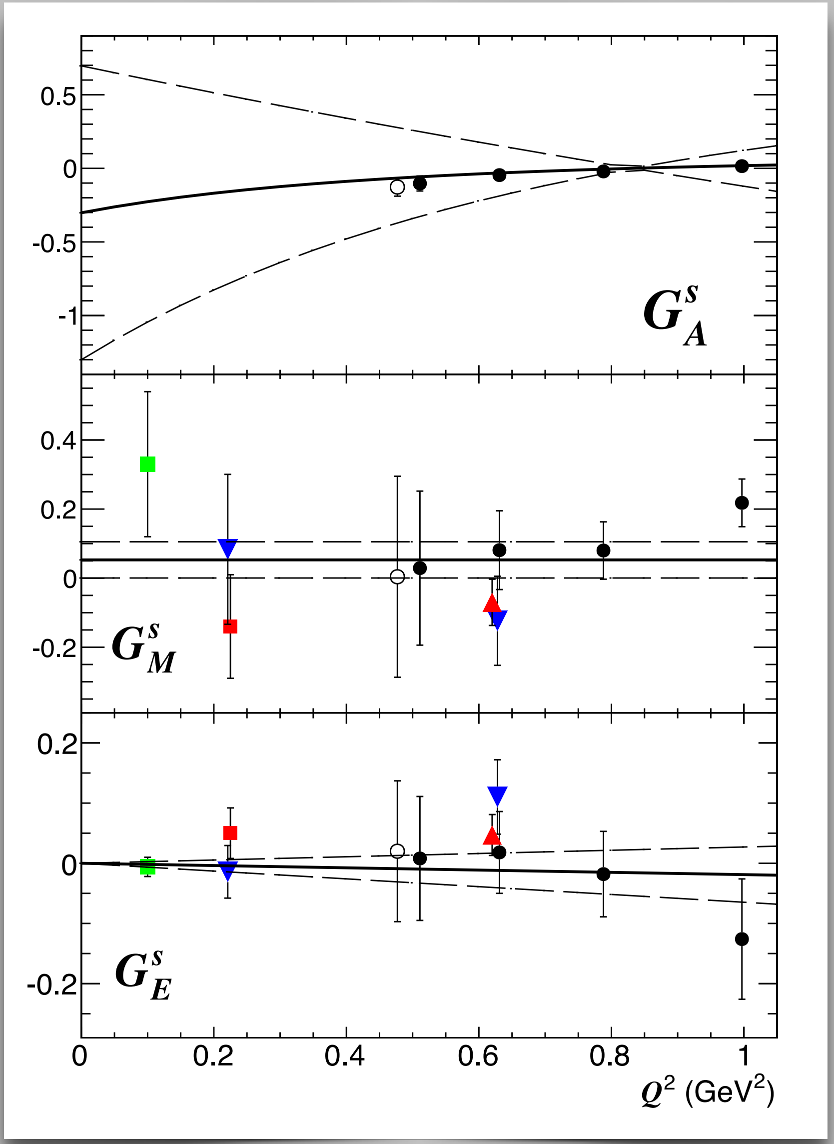

Weak Axial FF form e-p scattering

	$R_A^{T=1}$	$R_A^{T=0}$	$R_A^{(0)}$
one-quark	-0.172	-0.253	-0.551
many-quark	$-0.086(0.34)$	$0.014(0.19)$	N/A
total	$-0.258(0.34)$	$-0.239(0.20)$	$-0.55(0.55)$

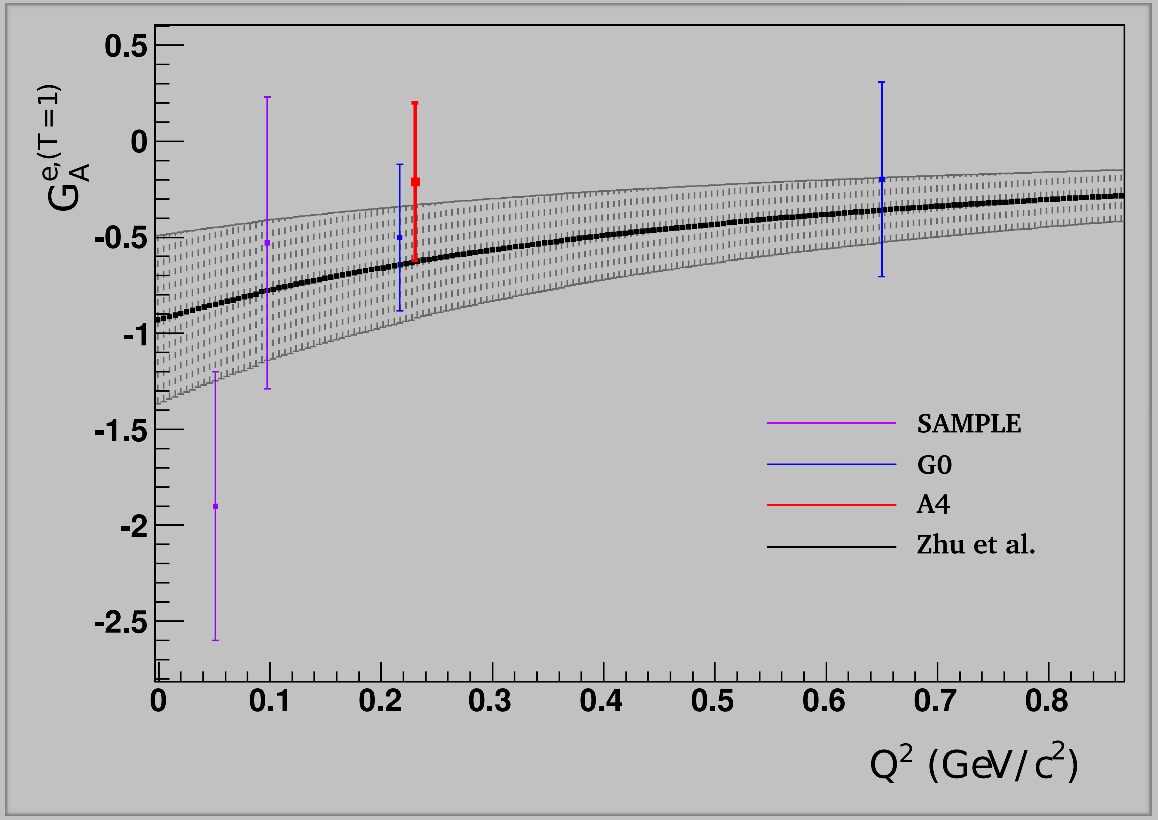

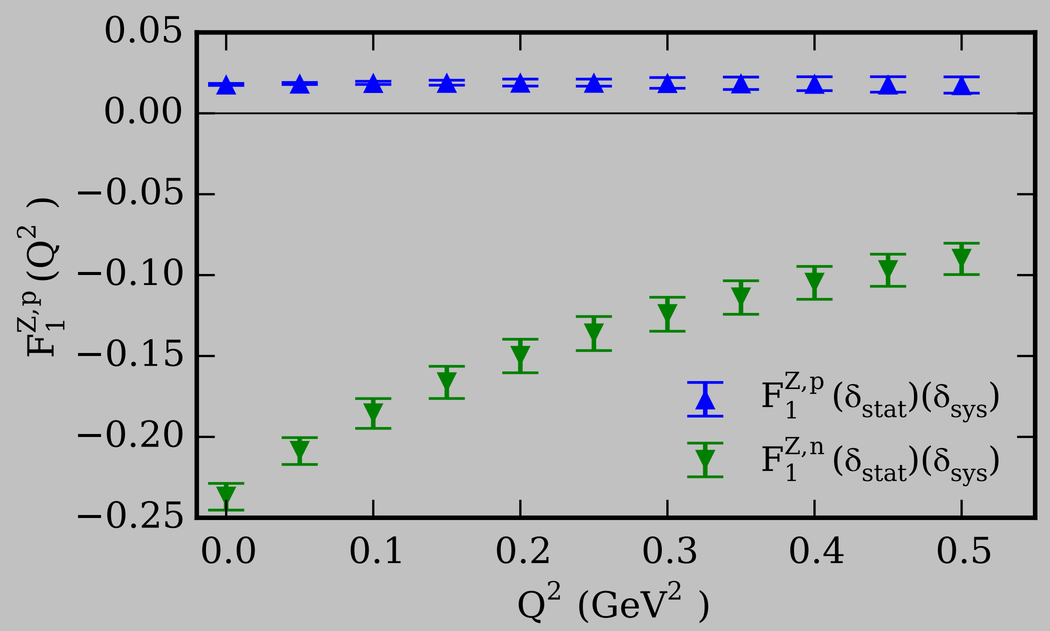

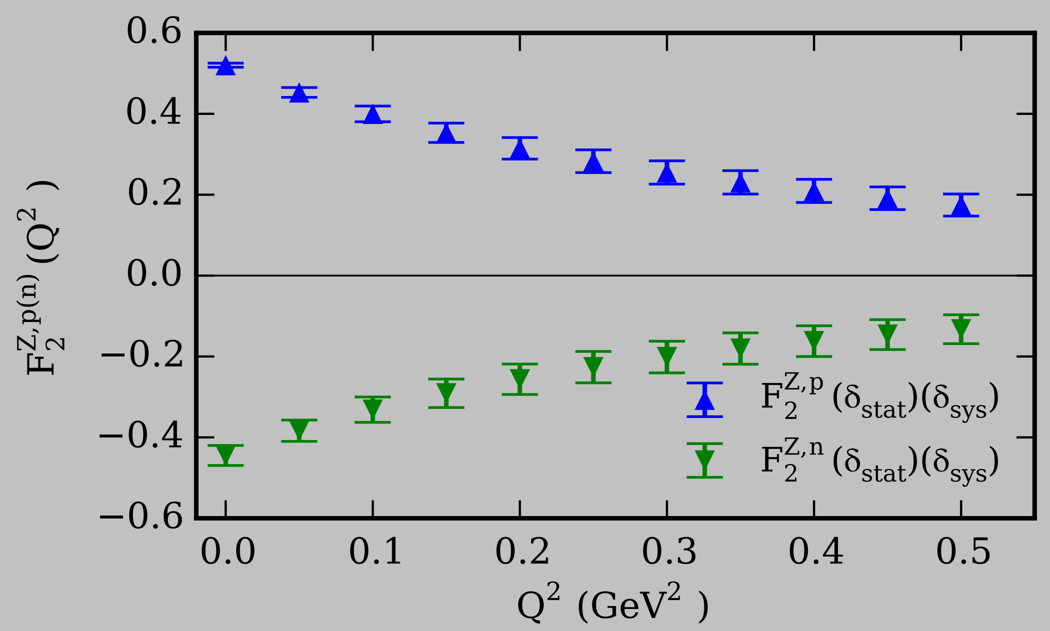

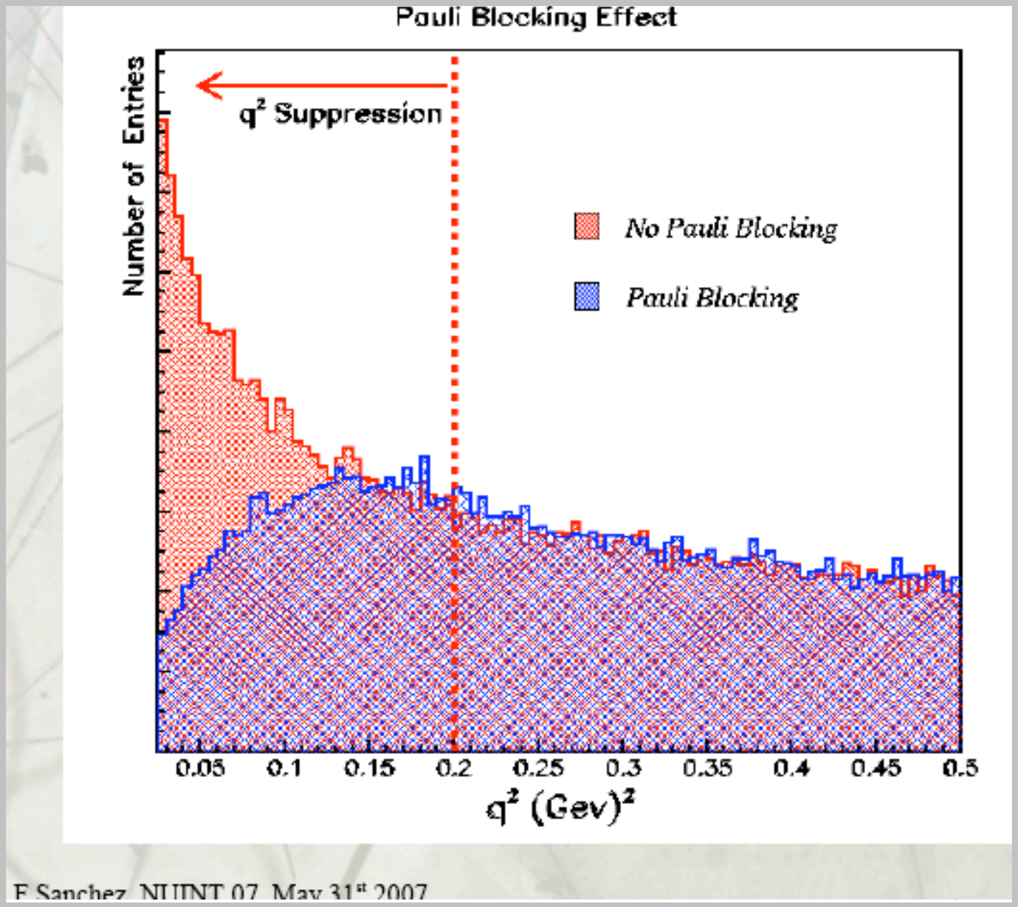

Particle	Lifetime (ns)	Decay mode	Branching ratio (%)
π^+	26.03	$\mu^+ + \nu_\mu$	99.9877
		$e^+ + \nu_e$	0.0123
K^+	12.385	$\mu^+ + \nu_\mu$	63.44
		$\pi^0 + e^+ + \nu_e$	4.98
		$\pi^0 + \mu^+ + \nu_\mu$	3.32
K_L^0	51.6	$\pi^- + e^+ + \nu_e$	20.333
		$\pi^+ + e^- + \overline{\nu}_e$	20.197
		$\pi^- + \mu^+ + \nu_\mu$	13.551
		$\pi^+ + \mu^- + \overline{\nu}_\mu$	13.469
μ^+	2197.03	$e^+ + \nu_e + \overline{\nu}_\mu$	100.0

Nucleon Electromagnetic FF (Connected Insertion Calculation)

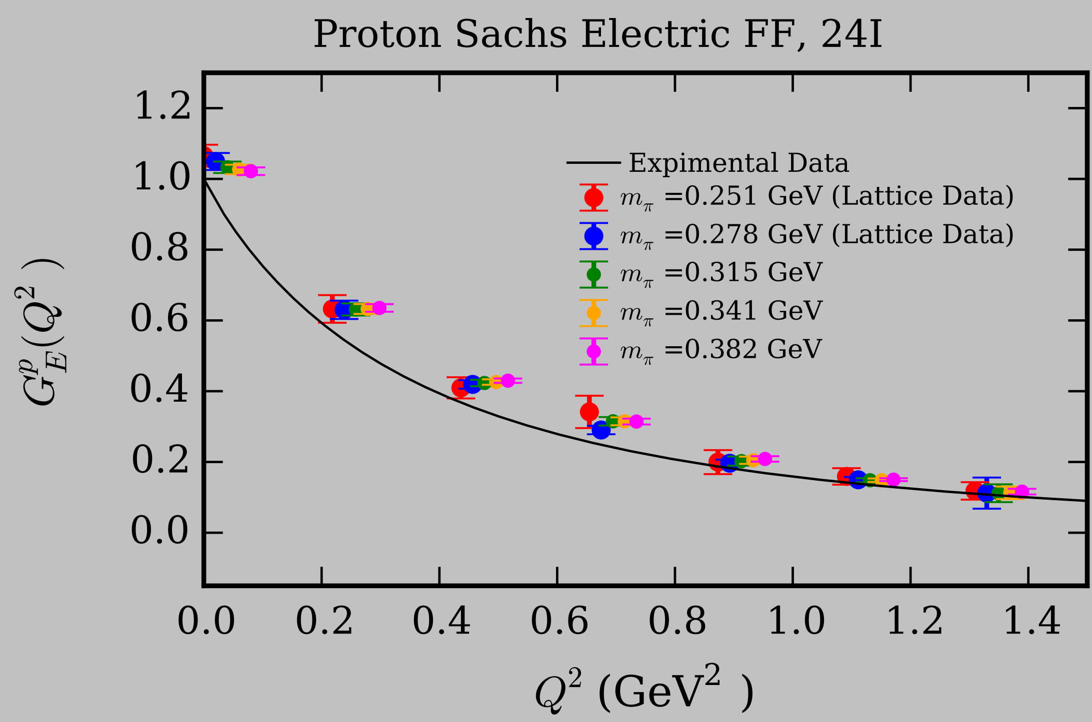

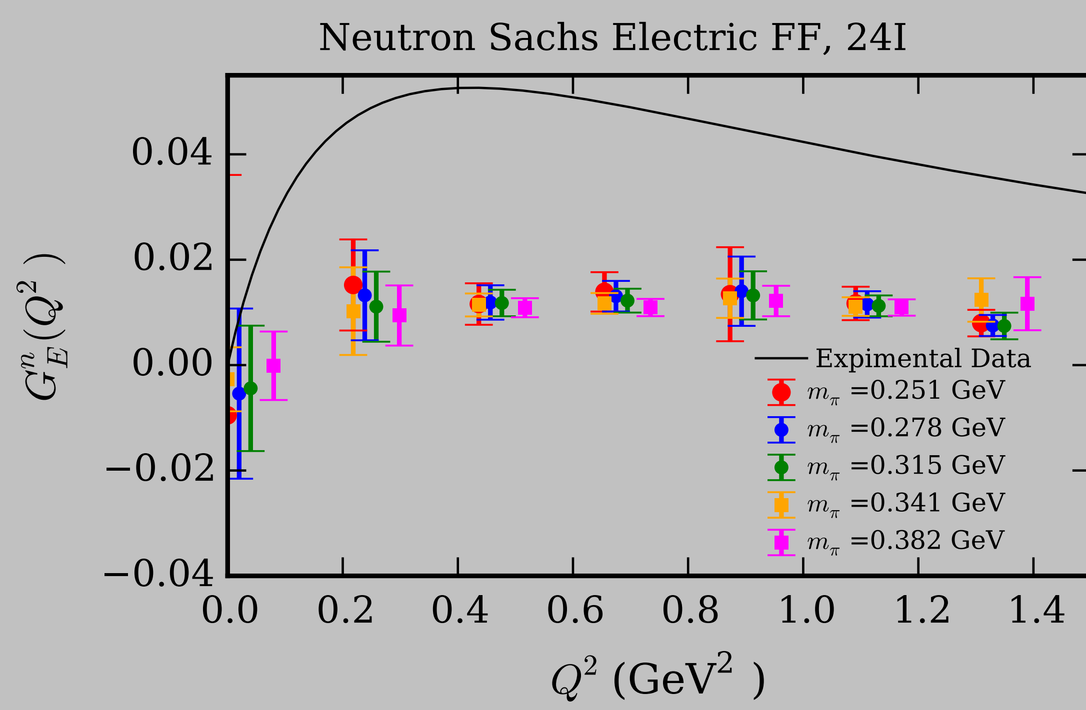

PHYSICAL REVIEW D **96,** 114504 (2017)

Sea quarks contribution to the nucleon magnetic moment and charge radius at the physical point

Raza Sabbir Sufian,[1] Yi-Bo Yang,[1,2] Jian Liang,[1] Terrence Draper,[1] and Keh-Fei Liu[1]

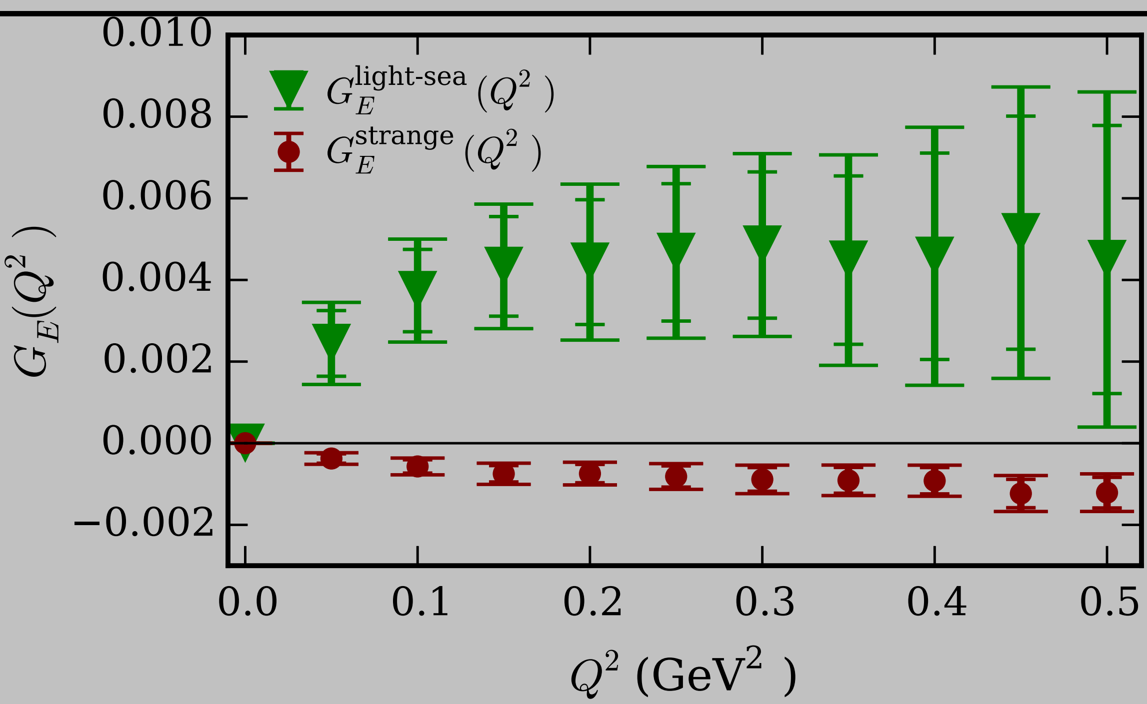

* Inclusion of DI will push nucleon total (CI +DI) electric EFFs in the right direction
But a little bit noisier

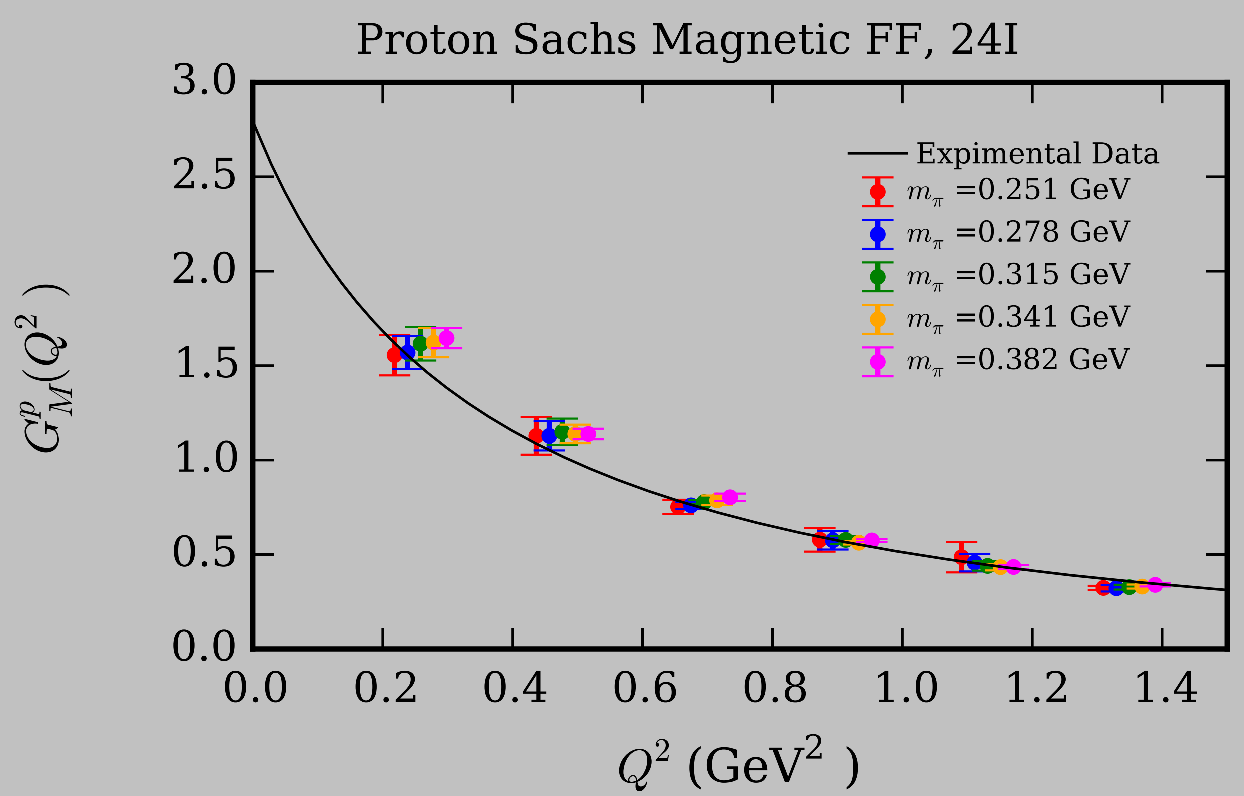

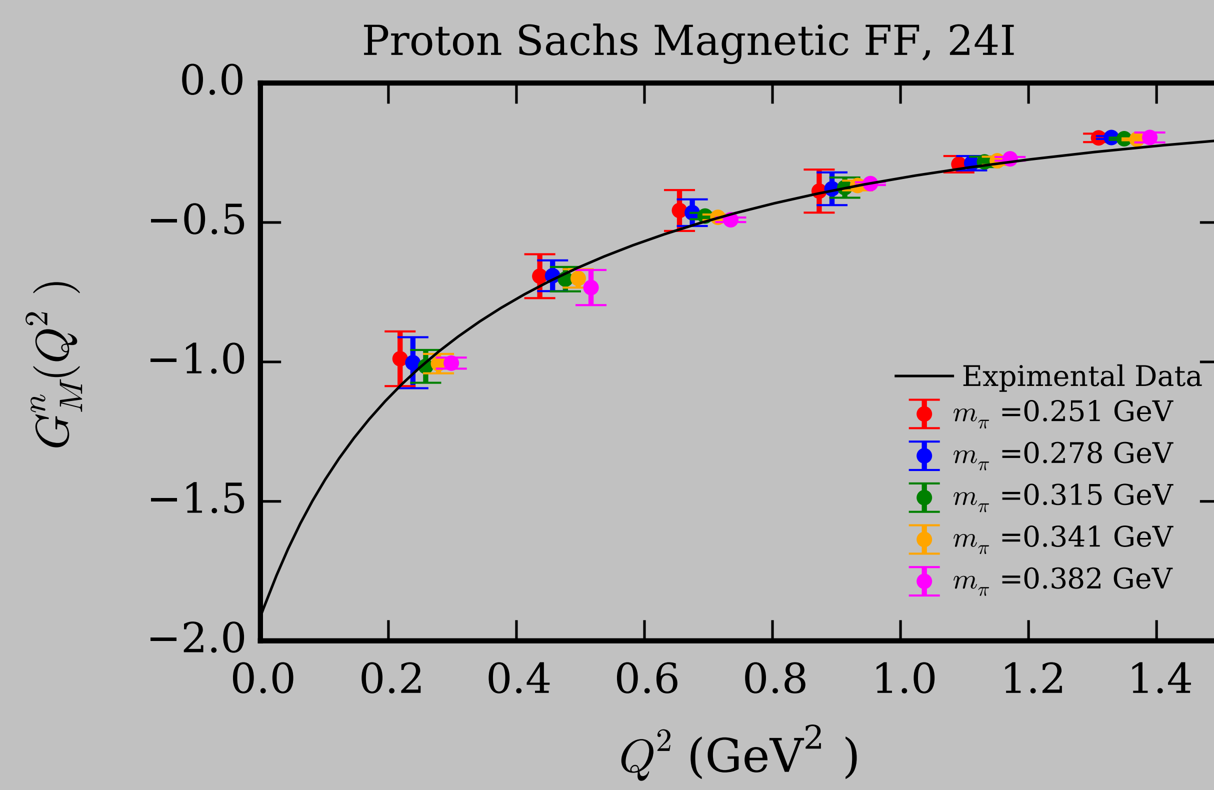

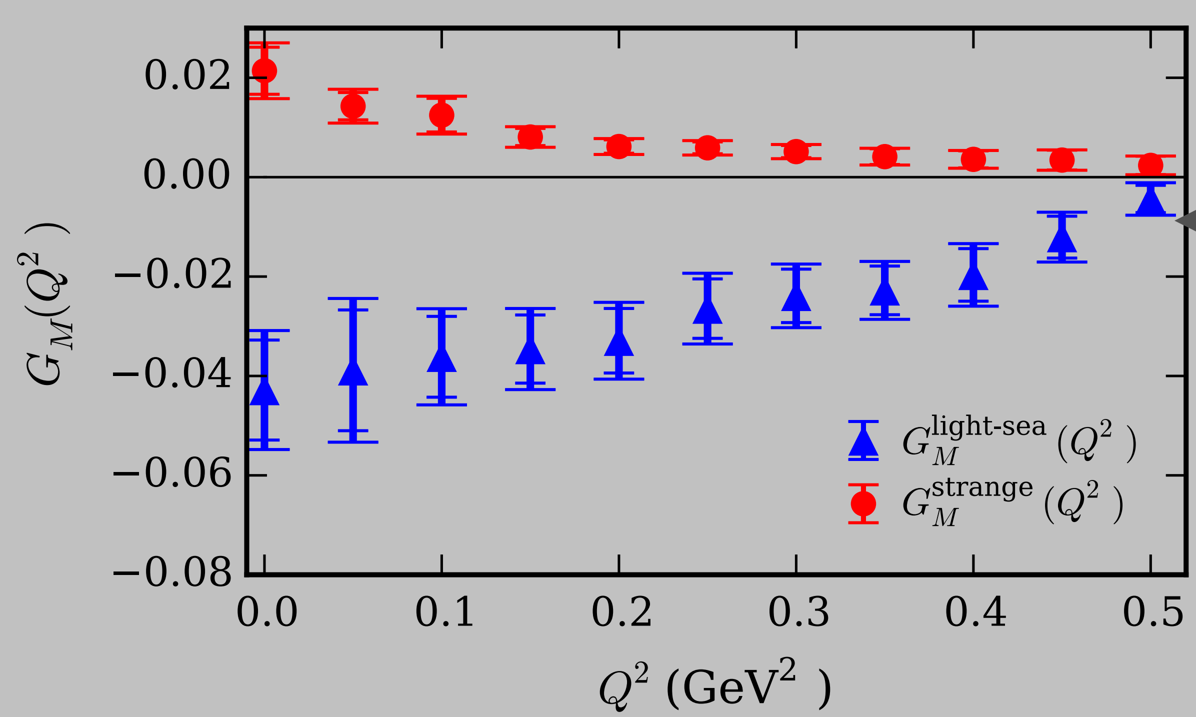

DI contribution

DI contribution to magnetic FF not very significant

Magnetic Moment Extrapolation

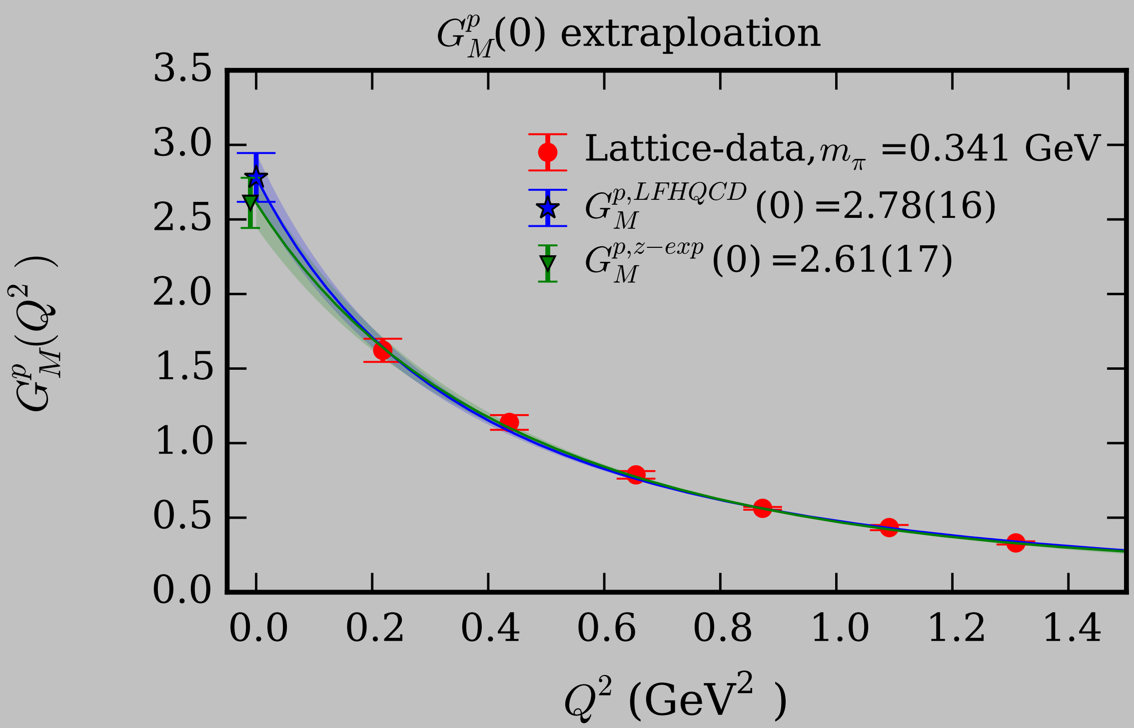

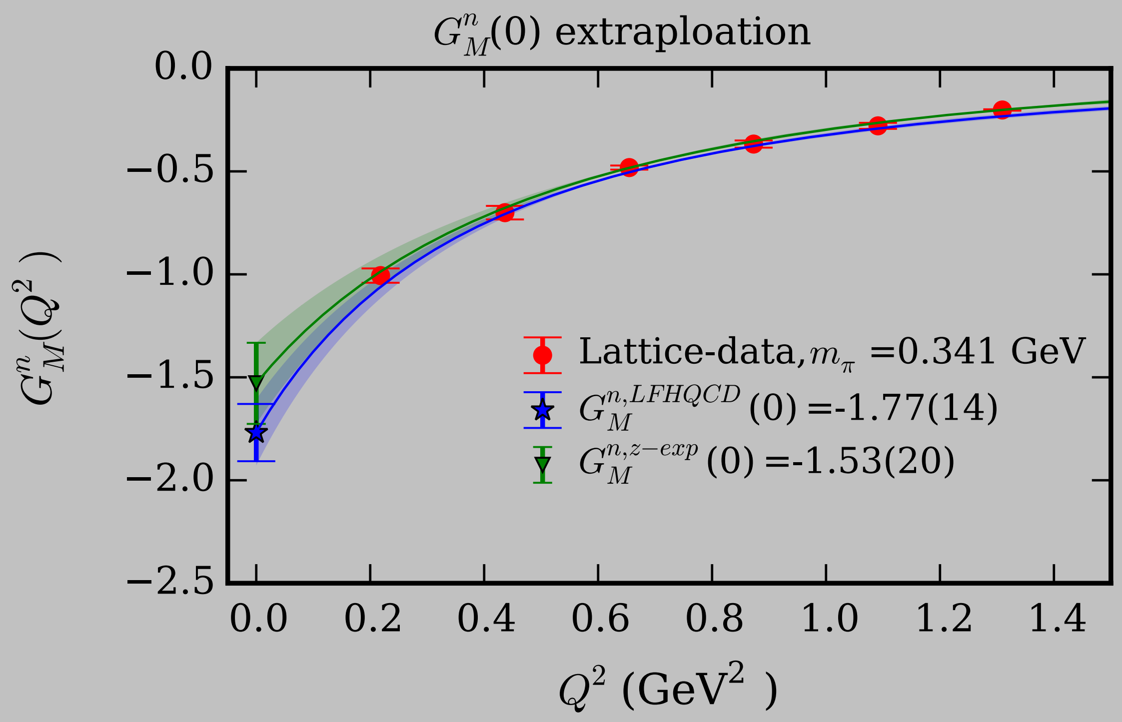

$$F_1^p(Q^2) = F_{i=3}(Q^2),$$

$$F_2^p(Q^2) = \chi_p[(1-\gamma_p)F_{i=4}(Q^2) + \gamma_p F_{i=6}(Q^2)]$$

$$F_\tau(Q^2) = \frac{1}{\left(1+\frac{Q^2}{M^2_{\rho_{n=0}}}\right)\left(1+\frac{Q^2}{M^2_{\rho_{n=1}}}\right)\cdots\left(1+\frac{Q^2}{M^2_{\rho_{n=\tau-2}}}\right)}$$

Sufian, de Teramond, Brodsky, Deur, Dosch

PHYSICAL REVIEW D **95,** 014011 (2017)

Analysis on 32I Ensemble

*Only 100 configs used for source-sink separation t=14

*No Fit, just average value at t = 8

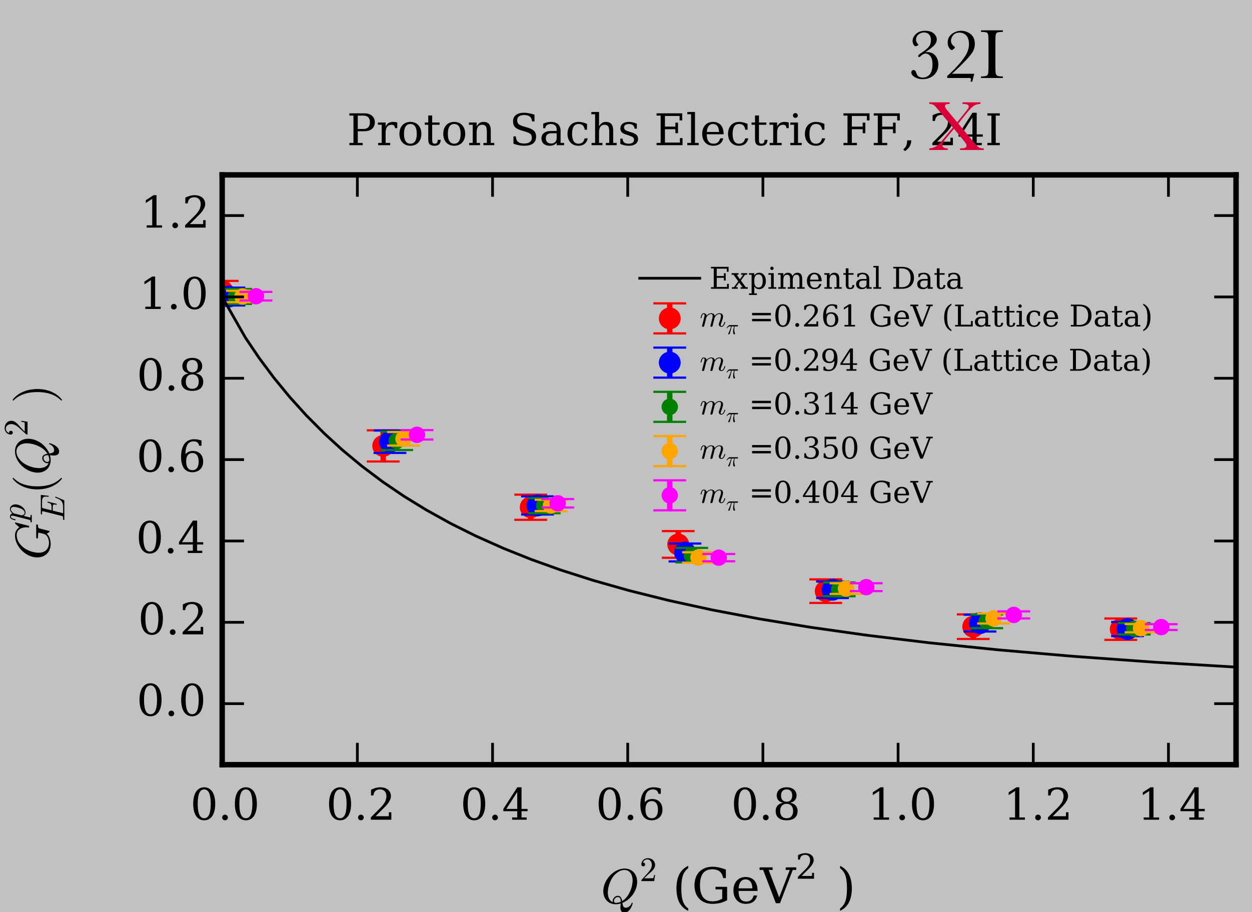

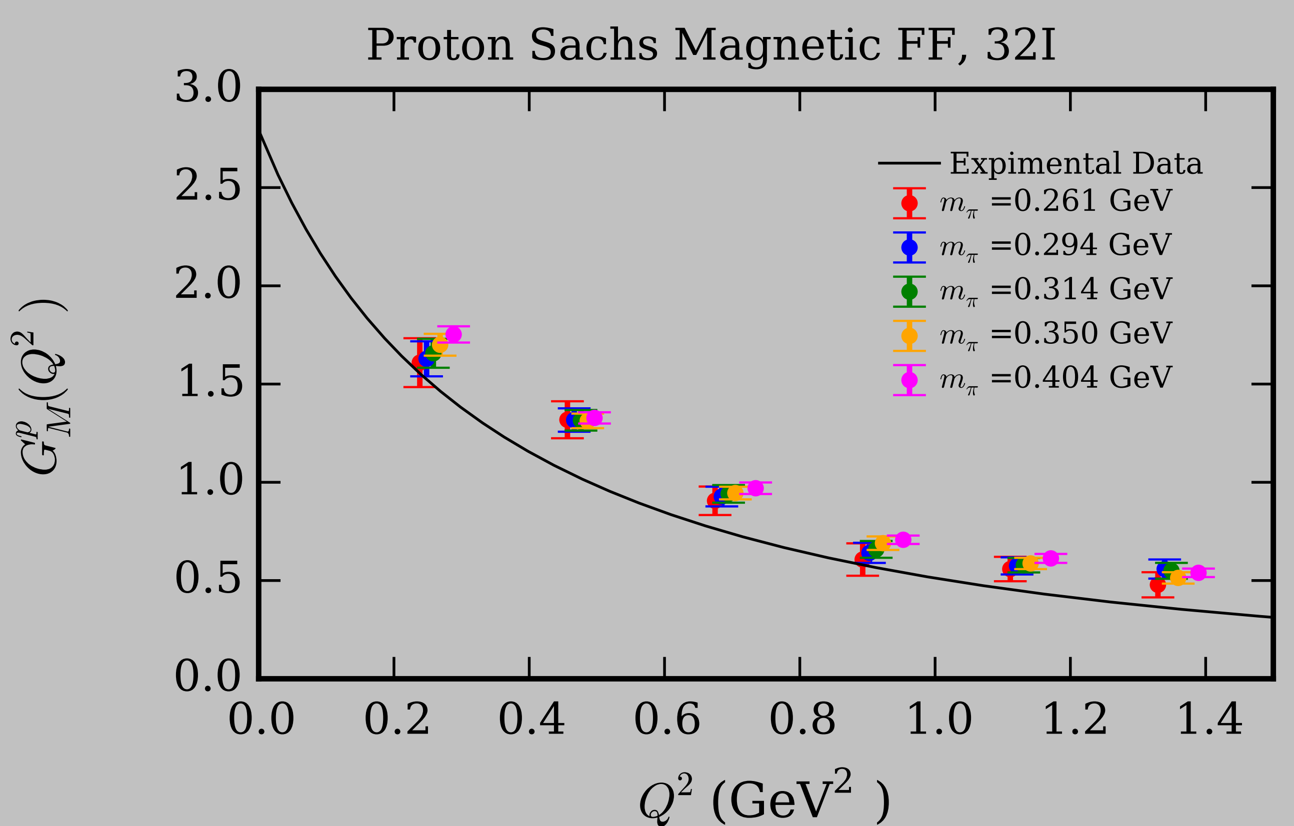

Some of many calculations

de Téramond, Liu, **RSS**, Dosch, Brodsky, Deur
PRL (2018)

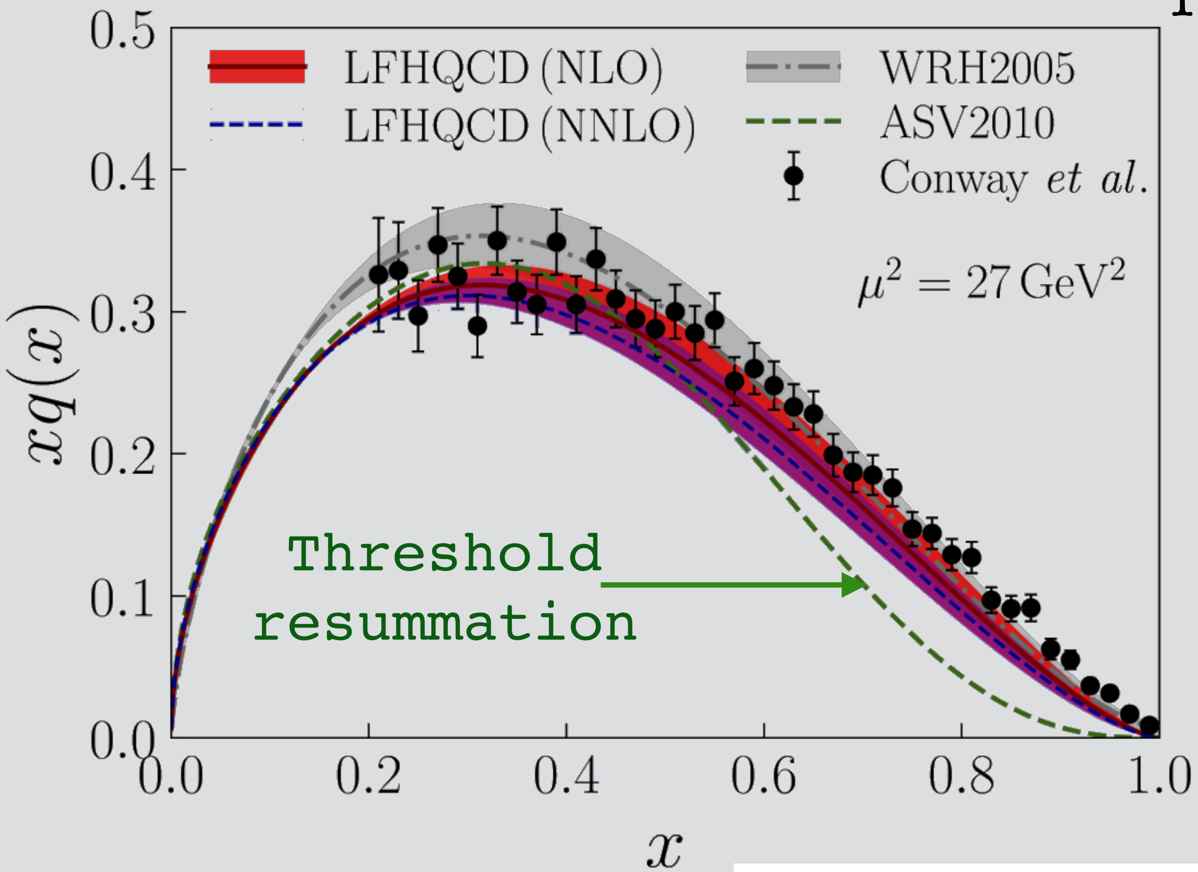

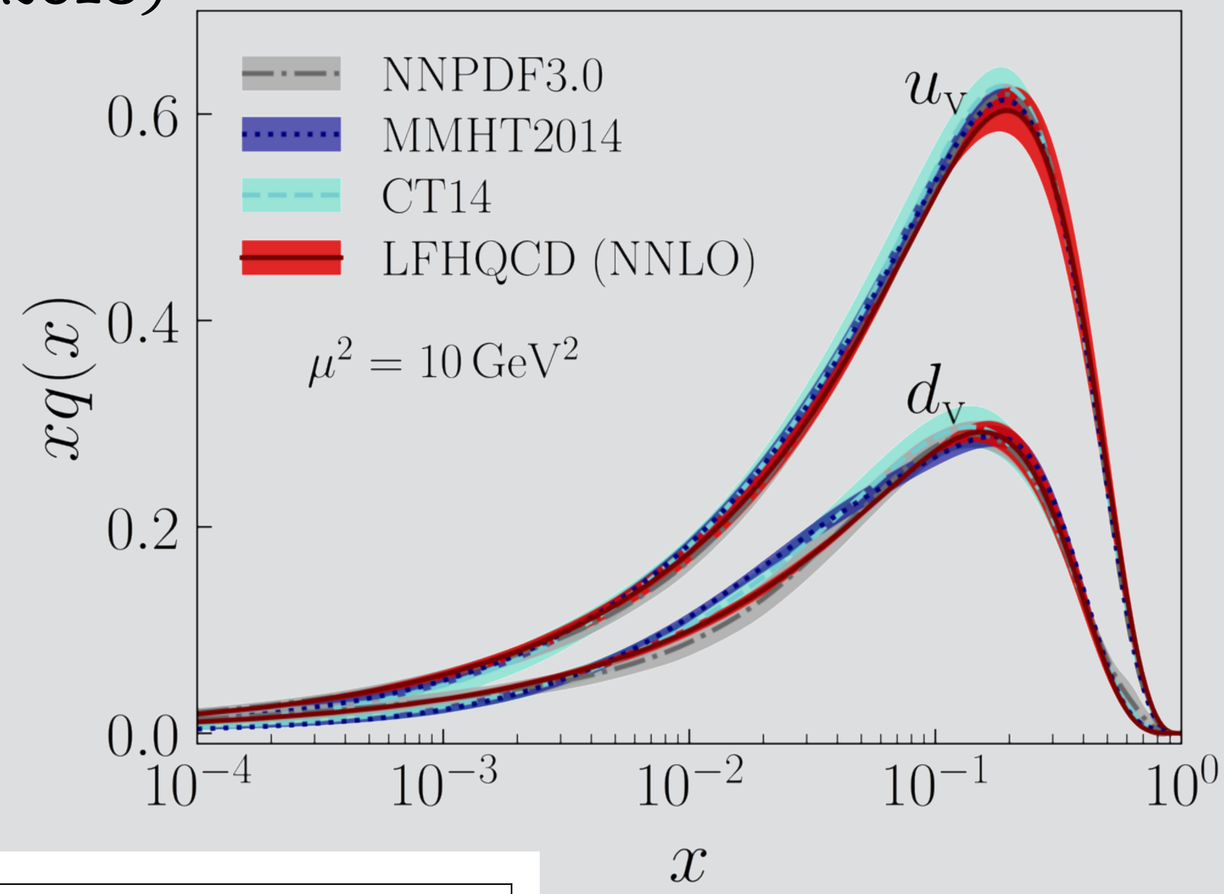

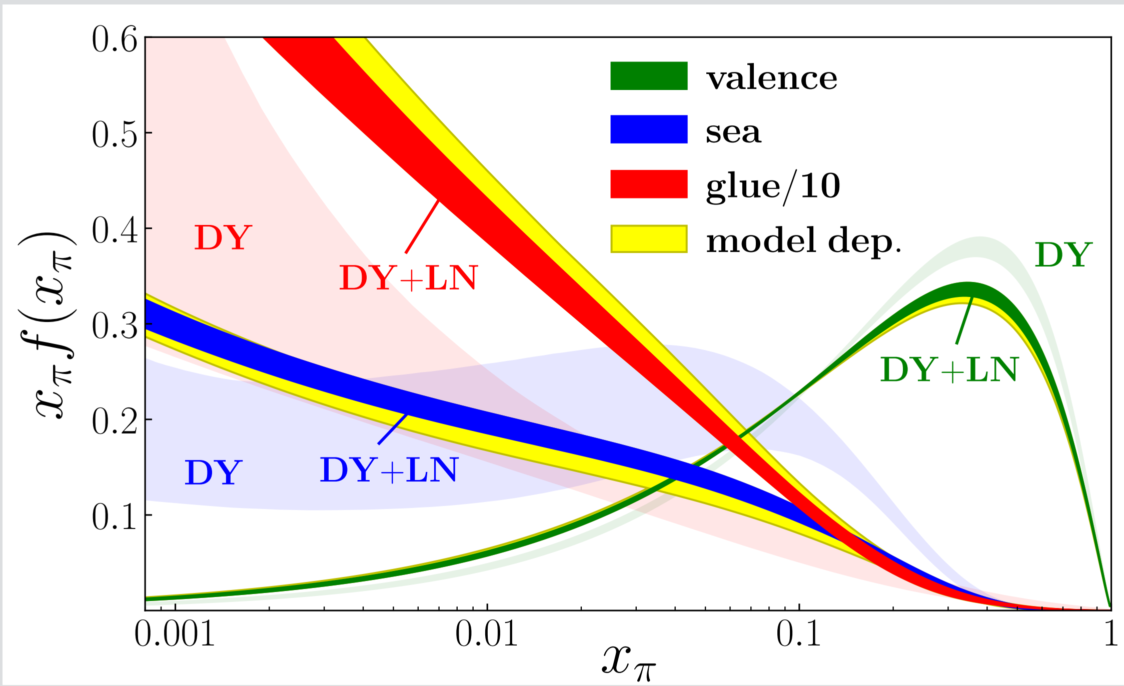

Barry, et. al. JAM Collaboration
to appear in PRL

Factorization Theorem

$$F_1\left(x, \frac{Q^2}{\Lambda^2_{QCD}}\right) = \sum_j \int_x^1 \frac{dy}{y} C_j\left(\frac{x}{y}, \frac{Q^2}{\mu^2}\right) f_j\left(y, \frac{\mu}{\Lambda_{QCD}}\right) + \mathcal{O}\left(\frac{\Lambda^2_{QCD}}{Q^2}\right)$$

x=momentum fraction of struck-quark

y=momentum fraction of parton j in proton

$$f_{q_i}\left(y, \frac{\mu}{\Lambda}\right) = \int \frac{\xi}{2\pi} e^{-2i(y\bar{n}\cdot P)\xi} < P|\bar{\psi}_i(\bar{n}\xi) W(\bar{n}\xi, -\bar{n}\xi) \not{\bar{n}} \psi_i(-\bar{n}\xi)|P >$$

$\bar{n}^2 = 0$ light cone matrix matrix element

$$W = P\, exp \int_{-\xi}^{\xi} ds\, \bar{n} \cdot A(\bar{n}s)$$

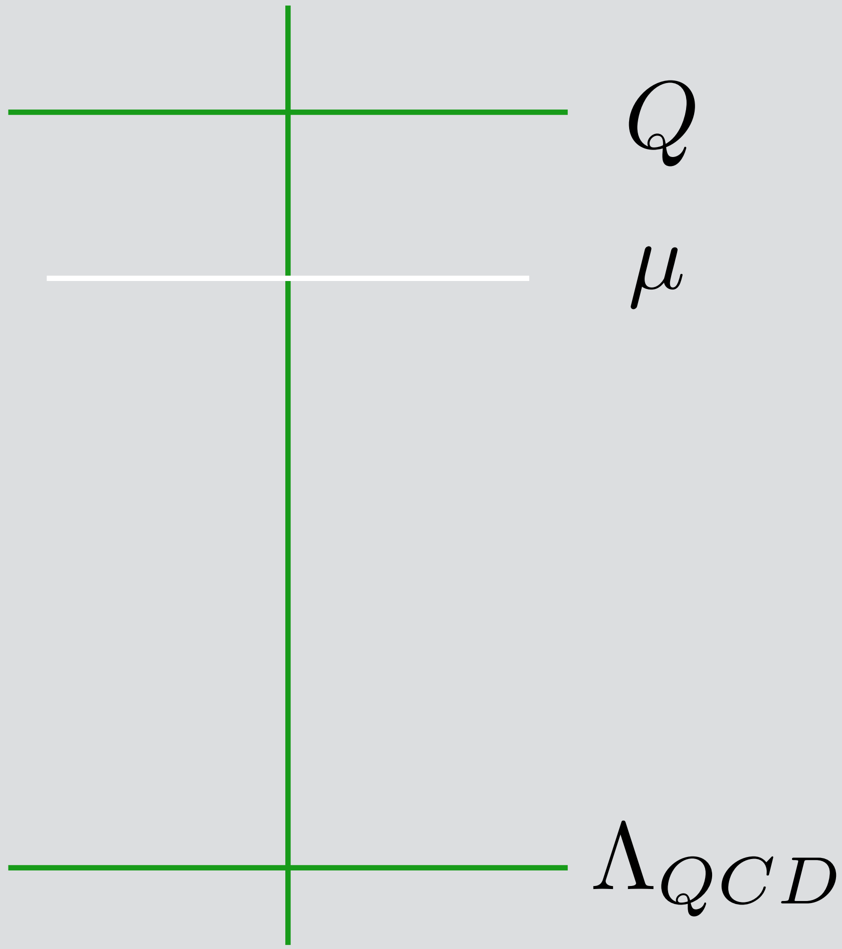

$$ln\left(\frac{Q}{\Lambda_{QCD}}\right) = ln\left(\frac{Q}{\mu}\right) + ln\left(\frac{\mu}{\Lambda_{QCD}}\right)$$

in C_j

in f_j

PDFs from DIS

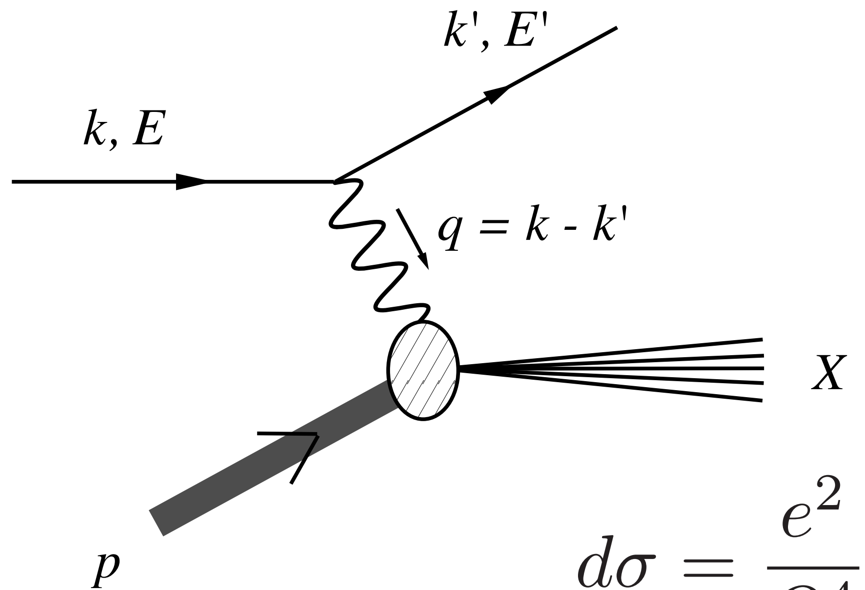

$$Q^2 = -q^2, \quad \nu = p \cdot q, \quad x = \frac{Q^2}{2\nu}$$

$$d\sigma = \frac{e^2}{Q^4} \int \frac{d^3k'}{(2\pi)^3 2E'} \frac{4\pi}{(2E)(2M)} l_{\mu\nu}(k,k') W^{\mu\nu}(p,q)$$

- Hadronic tensor

$$\begin{aligned} W_{\mu\nu}(p,q) &= \frac{1}{4\pi} \sum_X \langle p | j_\mu^\dagger(0) | X \rangle \langle X | j_\nu(0) | p \rangle (2\pi)^4 \delta(p_X - p - q) \\ &= \frac{1}{4\pi} \int d^4 y e^{iq\cdot y} \langle p | [j_\mu^\dagger(y), j_\nu(0)] | p \rangle \end{aligned}$$

- Leptonic tensor

$$l^{\mu\nu}(k,k') = [\bar{u}(k',\sigma')\gamma^\mu u(k,\sigma)]^* \bar{u}(k',\sigma')\gamma^\nu u(k,\sigma)$$

Pseudo-PDFs

[A. Radyushkin (2017)]

- Lorentz decomposition of matrix element

$$\begin{aligned} \mathcal{M}^\alpha(z,p) &= \langle p|\overline{\psi}(z)\gamma^\alpha W_z(z,0)\psi(0)|p\rangle \\ &= 2p^\alpha \mathcal{M}_p(-(zp),-z^2) + z^\alpha \mathcal{M}_z(-(zp),-z^2). \end{aligned}$$

- Light-cone

$$p = (p_+, 0, 0_\perp), \quad z = (0, z_-, 0_\perp)$$

$$\mathcal{M}^+(z,p) = 2p^+ \mathcal{M}_p(-p_+z_-, 0)$$

$$\mathcal{M}_p(-p_+z_-, 0) = \int_{-1}^{1} dx e^{-ixp_+z_-} f(x)$$

light-cone PDF

Ioffe time PDF

$\mathcal{M}_p(-zp, -z^2)$ Lorentz invariant. Computable in any frame.

$\nu = -pz$ Ioffe time [B. L. Ioffe (1969)]

$$\mathcal{M}_p(\nu, -z^2) = \int_{-1}^{1} dx e^{ix\nu} \mathcal{P}(x, -z^2).$$

Ioffe time PDF pseudo-PDF

Pseudo-PDF has $-1 \leq x \leq 1$ support. [A. Radyushkin (2017)]

$z^2 \to 0$ limit

$$\mathcal{M}_p(\nu, 0) = \int_{-1}^{1} dx e^{ix\nu} f(x) \qquad \left(\mathcal{M}_p(-p_+z_-, 0) = \int_{-1}^{1} dx e^{-ixp_+z_-} f(x)\right)$$

$$\mathcal{P}(x, -z^2) \xrightarrow[z^2 \to 0]{} f(x)$$

Quasi-PDF case

$$p = (E, 0_\perp, p_3), \quad z = (0, 0_\perp, z_3)$$

$$\mathcal{M}^3(z,p) \quad = \quad 2p^3 \mathcal{M}_p(-z_3 p_3, -z_3^2) + z^3 \mathcal{M}_z(-z_3 p_3, -z_3^2).$$

$$\begin{aligned}
\widetilde{q}(\tilde{x}, p_3) &= \frac{1}{2\pi}\int_{-\infty}^{\infty} dz e^{-i\tilde{x}p_3 z}\mathcal{M}^3(z,p) \\
&= \frac{1}{2\pi}\int_{-\infty}^{\infty} d\nu e^{-i\tilde{x}\nu}\left[\mathcal{M}_p(\nu, \nu^2/p_3^2) - \frac{\nu}{2p_3^2}\mathcal{M}_z(\nu, \nu^2/p_3^2)\right].
\end{aligned}$$

$$\widetilde{q}(x, p_3) \xrightarrow[p_3 \to \infty]{} f(x)$$

Better choice

$$\mathcal{M}^0(z,p) \quad = \quad 2p^0 \mathcal{M}_p(-z_3 p_3, -z_3^2).$$

$$\widetilde{q}'(\tilde{x}, p_3) = \frac{1}{2\pi}\int_{-\infty}^{\infty} dz e^{-i\tilde{x}p_3 z}\mathcal{M}^0(z,p) = \frac{1}{2\pi}\int_{-\infty}^{\infty} d\nu e^{-i\tilde{x}\nu}\mathcal{M}_p(\nu, \nu^2/p_3^2).$$

Ratio

$$\mathfrak{M}(\nu, z_3^2) = \frac{\mathcal{M}_p(\nu, z_3^2)}{\mathcal{M}_p(0, z_3^2)}$$

$$\mathcal{M}_p(0, z_3^2) \xrightarrow[z_3^2 \to 0]{} 1$$ regular in the limit

By taking the ratio:
- smaller scaling violation in $z_3 \to 0$
- power divergence is canceled and well defined in taking continuum limit

Scale evolution (DGLAP)

different z_3^2 ⟷ different scale

$$\frac{d}{d \ln z_3^2} \mathcal{M}(\nu, z_3^2) = -\frac{\alpha_s}{2\pi} C_F \int_0^1 du B(u) \mathcal{M}(u\nu, z_3^2), \quad B(u) = \left[\frac{1+u^2}{1-u}\right]_+$$

Pseudo v.s. Quasi

- By taking the ratio, pseudo-PDF is better for renormalization.
- Small-x region requires large $\nu = -pz$; eventually large momentum data is required (?)

$$\mathcal{M}_p(\nu, -z^2) = \int_{-1}^{1} dx e^{ix\nu} \mathcal{P}(x, -z^2).$$

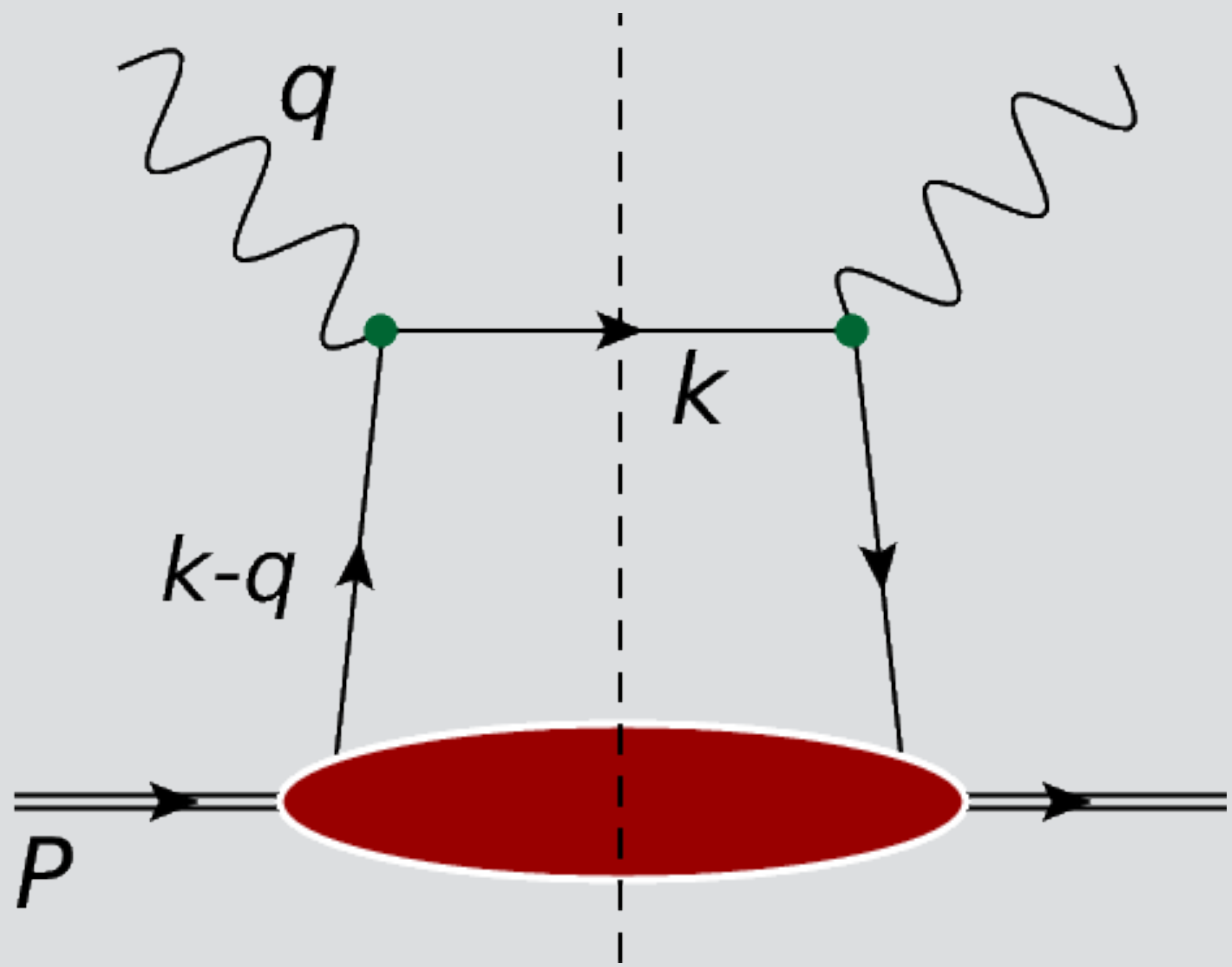
q
k
k-q
P

❑ DIS cross section is infrared divergent, and nonperturbative!

$$\sigma^{\mathrm{DIS}}_{\ell p\to\ell' X(\mathrm{everything})} \propto$$

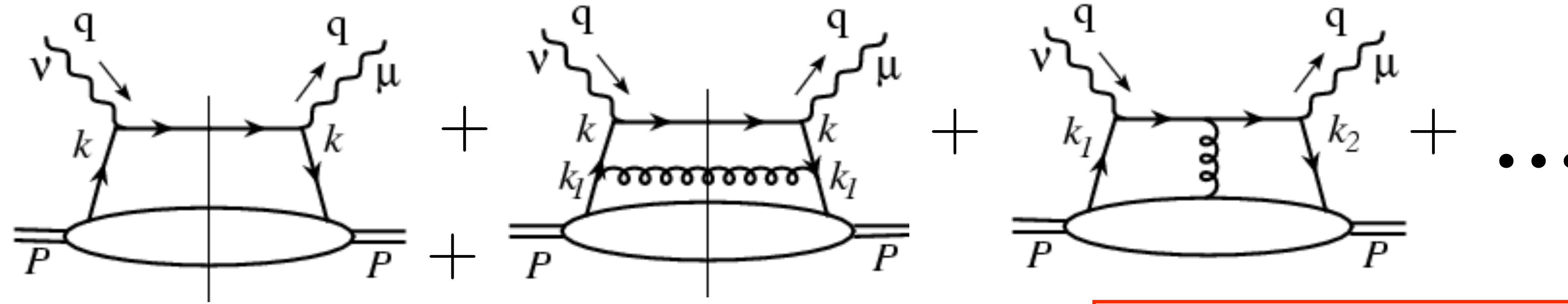

❑ QCD factorization (approximation!)

Color entanglement
Approximation

$$\sigma^{\mathrm{DIS}}_{\ell p\to\ell' X(\mathrm{everything})} =$$

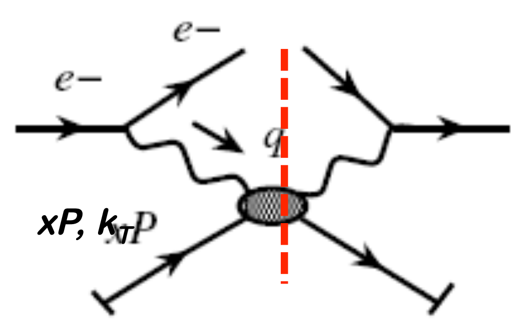

$$\otimes$$

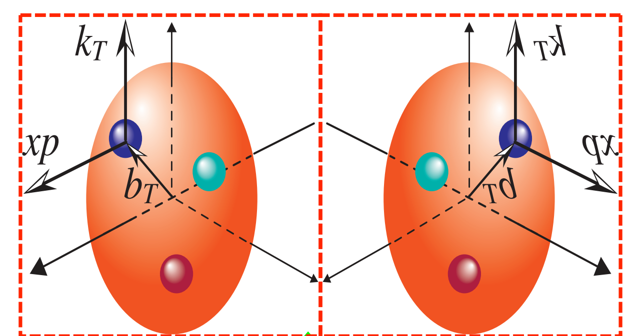

$$+\ O\left(\frac{1}{QR}\right)$$

Physical
Observable

Controllable
Probe

Quantum Probabilities
Structure

Quasi-Distribution of Pion

$m_\pi \simeq 300\,\mathrm{MeV}$

LP3, arXiv:1804.01483

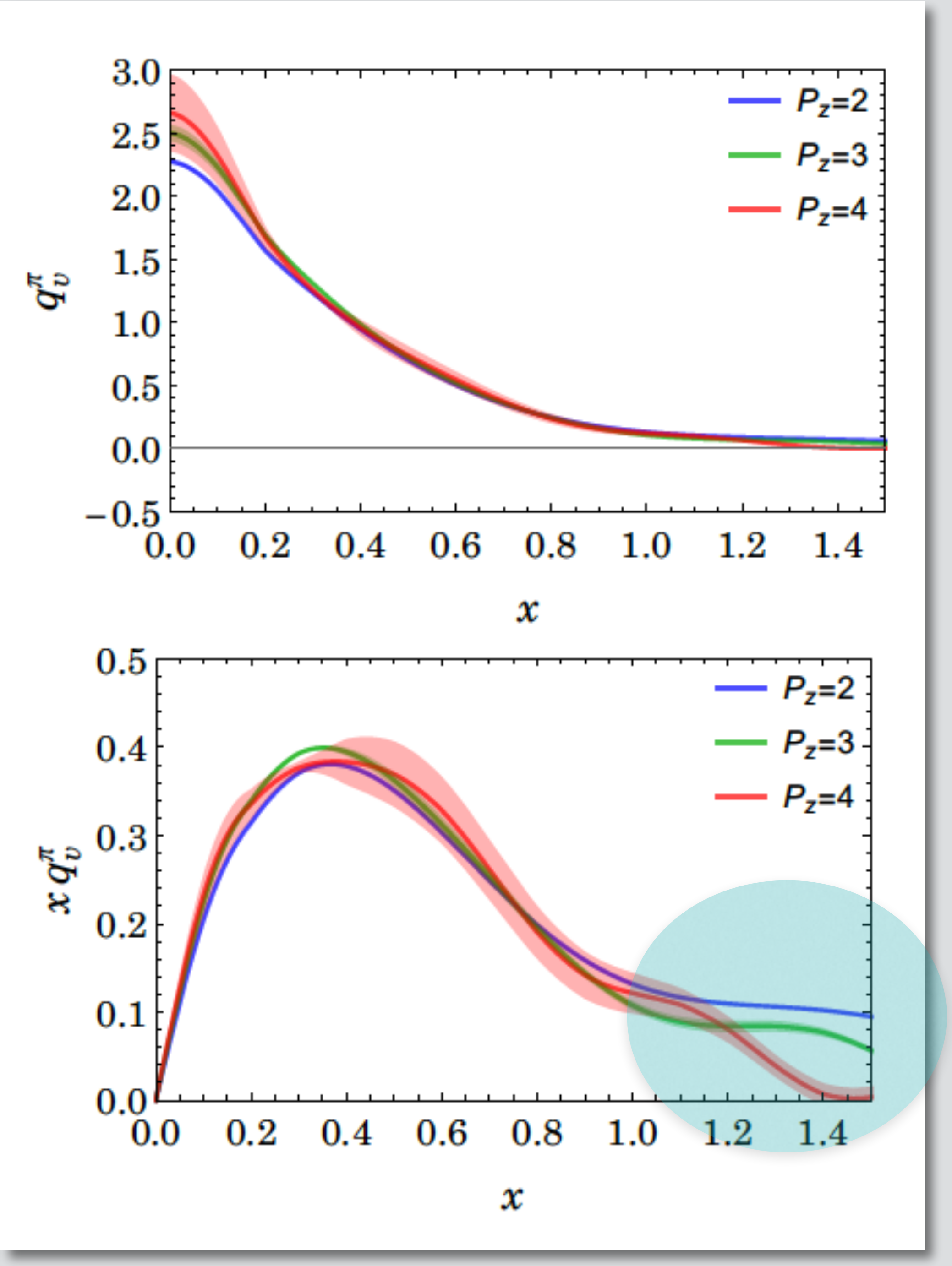

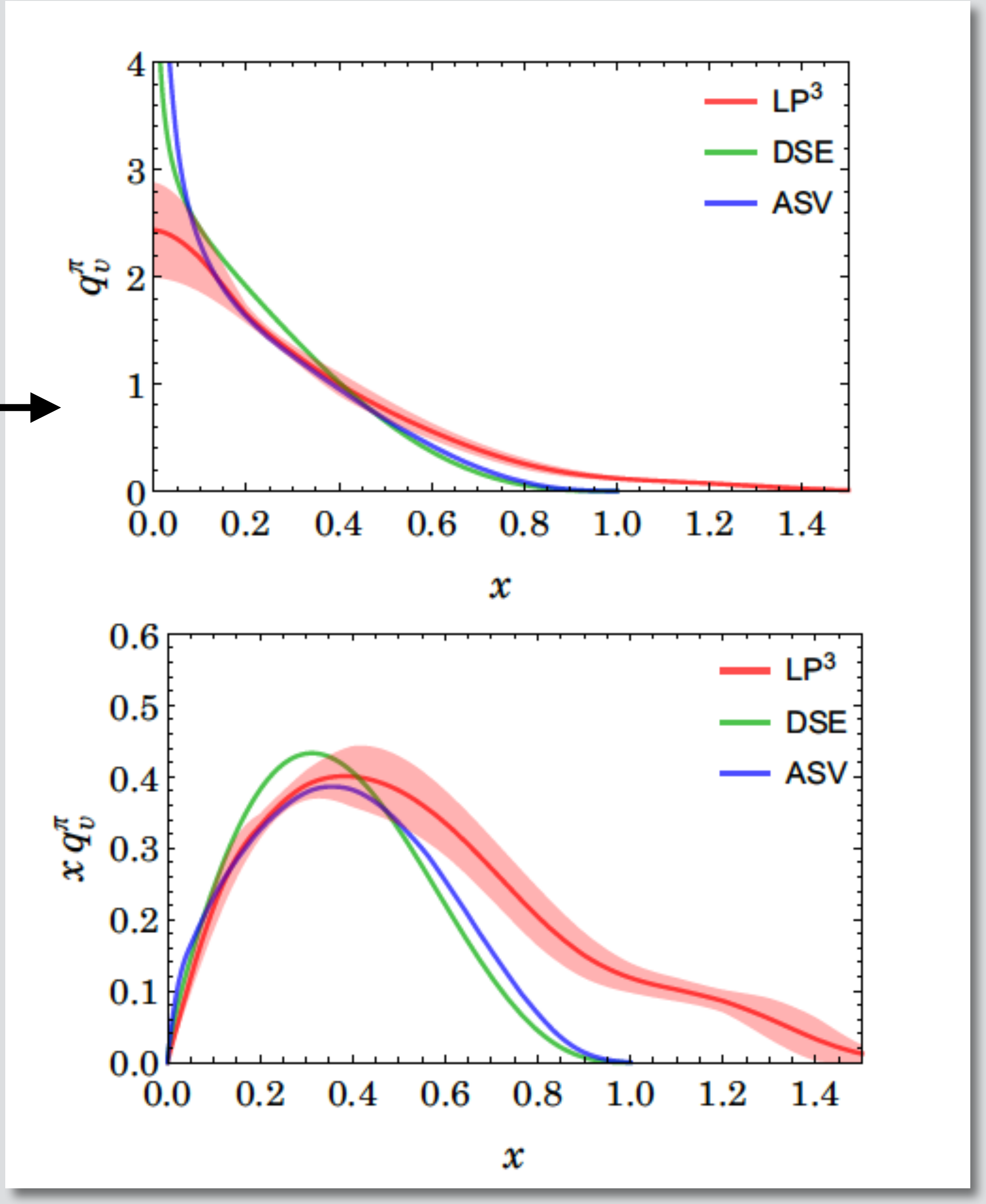

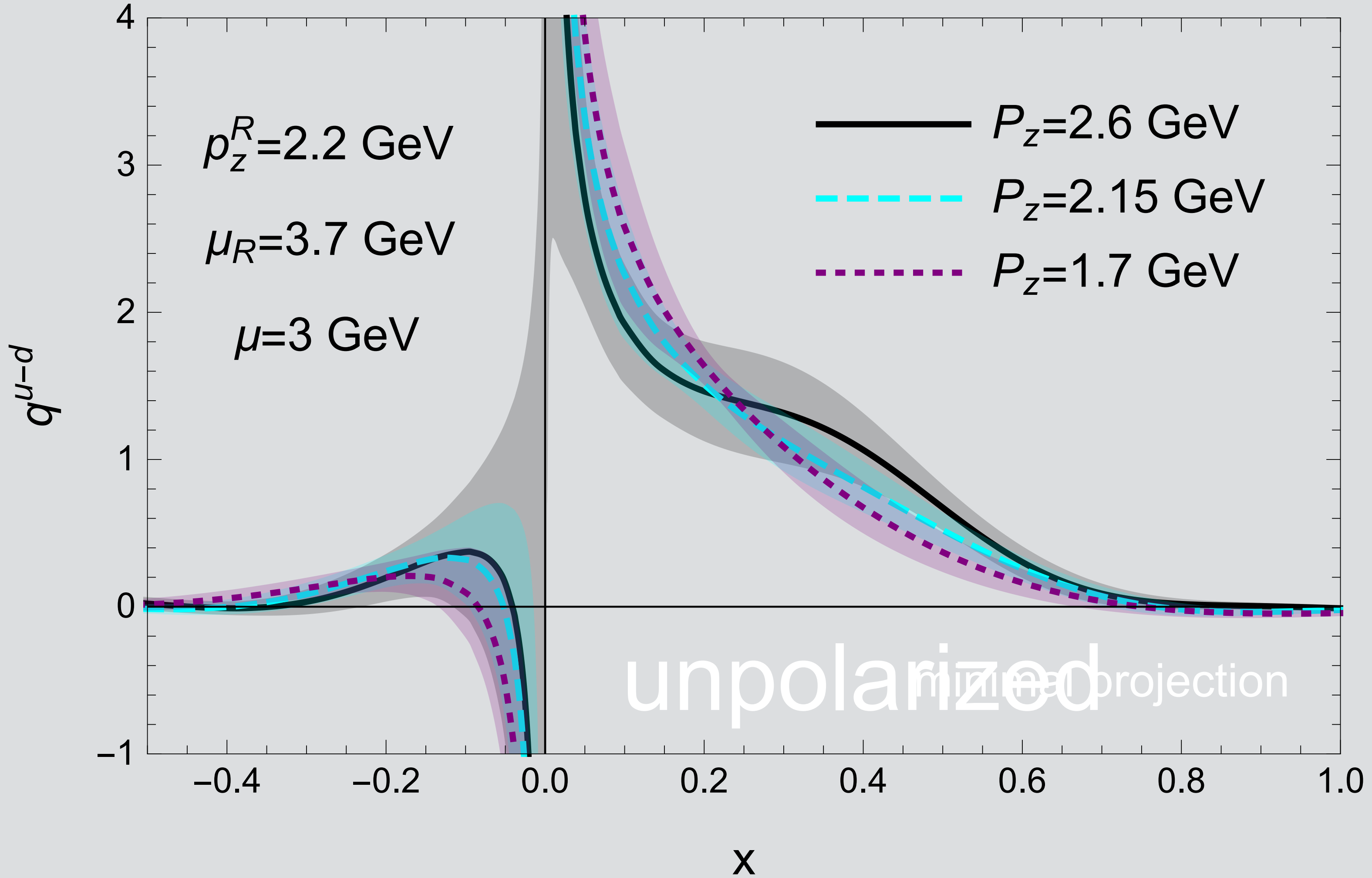

p_z^R=2.2 GeV
μ_R=3.7 GeV
μ=3 GeV
P_z=2.6 GeV
P_z=2.15 GeV
P_z=1.7 GeV
unpolarized
minimal projection
q^{u-d}
x

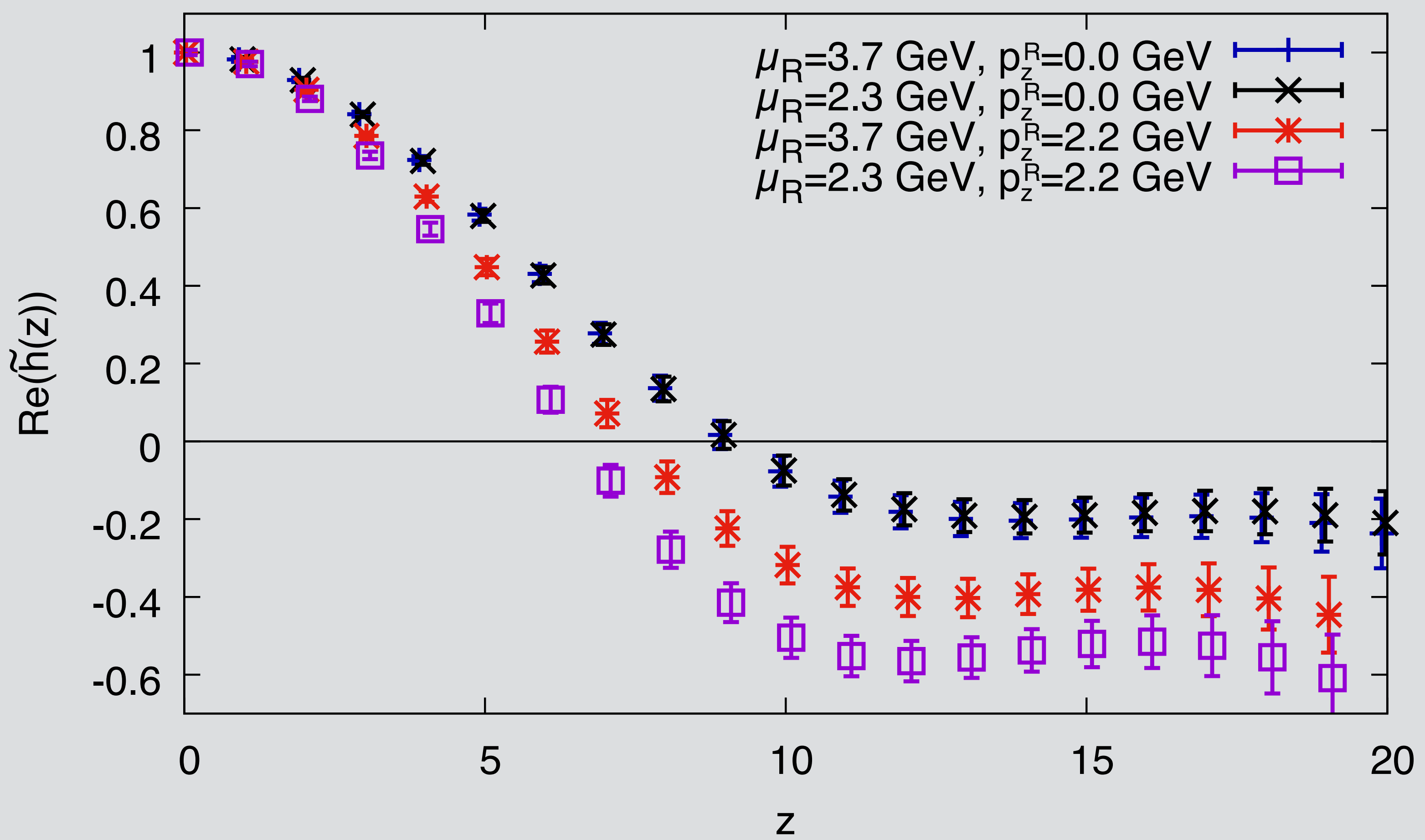

μ_R=3.7 GeV, p_z^R=0.0 GeV
μ_R=2.3 GeV, p_z^R=0.0 GeV
μ_R=3.7 GeV, p_z^R=2.2 GeV
μ_R=2.3 GeV, p_z^R=2.2 GeV
Re($\tilde{h}$(z))
z

where

$$\tilde{f}_\alpha(x,\rho) = \frac{\alpha_s C_F}{2\pi}\begin{cases} \frac{x-\rho}{(1-x)(1-\rho)} + \frac{2x(2-x)-\rho(1+x)}{2(1-x)(1-\rho)^{3/2}} \ln\frac{2x-1+\sqrt{1-\rho}}{2x-1-\sqrt{1-\rho}} & x>1 \\ \frac{-3x+2x^2+\rho}{(1-x)(1-\rho)} + \frac{2x(2-x)-\rho(1+x)}{2(1-x)(1-\rho)^{3/2}} \ln\frac{1+\sqrt{1-\rho}}{1-\sqrt{1-\rho}} & 0<x<1 \\ -\frac{x-\rho}{(1-x)(1-\rho)} - \frac{2x(2-x)-\rho(1+x)}{2(1-x)(1-\rho)^{3/2}} \ln\frac{2x-1+\sqrt{1-\rho}}{2x-1-\sqrt{1-\rho}} & x<0 \end{cases}$$
$$+ \frac{\alpha_s C_F}{2\pi}(1-\tau)\begin{cases} \frac{\rho(-3x+2x^2+\rho)}{2(1-x)(1-\rho)(4x-4x^2-\rho)} + \frac{-\rho}{4(1-\rho)^{3/2}} \ln\frac{2x-1+\sqrt{1-\rho}}{2x-1-\sqrt{1-\rho}} & x>1 \\ \frac{-x+\rho}{2(1-x)(1-\rho)} + \frac{-\rho}{4(1-\rho)^{3/2}} \ln\frac{1+\sqrt{1-\rho}}{1-\sqrt{1-\rho}} & 0<x<1 \\ -\frac{\rho(-3x+2x^2+\rho)}{2(1-x)(1-\rho)(4x-4x^2-\rho)} - \frac{-\rho}{4(1-\rho)^{3/2}} \ln\frac{2x-1+\sqrt{1-\rho}}{2x-1-\sqrt{1-\rho}} & x<0 \end{cases}, \tag{44}$$

$$\tilde{f}_z(x,\rho) = \frac{\alpha_s C_F}{2\pi}\begin{cases} \frac{-2\rho(1-7x+6x^2)-\rho^2(1+2x)}{(1-\rho)^2(4x-4x^2-\rho)} g_{z\alpha} + \frac{4x(1-3x+2x^2)-\rho(2-11x+12x^2-4x^3)-\rho^2}{(1-x)(1-\rho)^2(4x-4x^2-\rho)} \\ \quad + \left[\frac{\rho(4-6x-\rho)}{2(1-\rho)^{5/2}} g_{z\alpha} + \frac{2-4x+4x^2-5x\rho+2x^2\rho+\rho^2}{2(1-x)(1-\rho)^{5/2}}\right] \ln\frac{2x-1+\sqrt{1-\rho}}{2x-1-\sqrt{1-\rho}} & x>1 \\ \frac{-2+2x-\rho(1-4x)}{(1-\rho)^2} g_{z\alpha} + \frac{(-1+2x)(2-3x+\rho)}{(1-x)(1-\rho)^2} \\ \quad + \left[\frac{\rho(4-6x-\rho)}{2(1-\rho)^{5/2}} g_{z\alpha} + \frac{2-4x+4x^2-5x\rho+2x^2\rho+\rho^2}{2(1-x)(1-\rho)^{5/2}}\right] \ln\frac{1+\sqrt{1-\rho}}{1-\sqrt{1-\rho}} & 0<x<1 \\ -\frac{-2\rho(1-7x+6x^2)-\rho^2(1+2x)}{(1-\rho)^2(4x-4x^2-\rho)} g_{z\alpha} - \frac{4x(1-3x+2x^2)-\rho(2-11x+12x^2-4x^3)-\rho^2}{(1-x)(1-\rho)^2(4x-4x^2-\rho)} \\ \quad - \left[\frac{\rho(4-6x-\rho)}{2(1-\rho)^{5/2}} g_{z\alpha} + \frac{2-4x+4x^2-5x\rho+2x^2\rho+\rho^2}{2(1-x)(1-\rho)^{5/2}}\right] \ln\frac{2x-1+\sqrt{1-\rho}}{2x-1-\sqrt{1-\rho}} & x<0 \end{cases}$$
$$+ \frac{\alpha_s C_F}{2\pi}(1-\tau)\begin{cases} \frac{\rho(1-2x)[-4x(1-x)(2+\rho)+3\rho^2]}{2(1-\rho)^2(4x-4x^2-\rho)^2} g_{z\alpha} + \frac{\rho[-4x(2-9x+6x^2)+\rho(1-10x+2\rho)]}{2(1-\rho)^2(4x-4x^2-\rho)^2} \\ \quad + \frac{\rho[(2+\rho)g_{z\alpha}+3)]}{4(1-\rho)^{5/2}} \ln\frac{2x-1+\sqrt{1-\rho}}{2x-1-\sqrt{1-\rho}} & x>1 \\ \frac{-3\rho g_{z\alpha}-1-2\rho}{2(1-\rho)^2} + \frac{\rho[(2+\rho)g_{z\alpha}+3)]}{4(1-\rho)^{5/2}} \ln\frac{1+\sqrt{1-\rho}}{1-\sqrt{1-\rho}} & 0<x<1 \\ -\frac{\rho(1-2x)[-4x(1-x)(2+\rho)+3\rho^2]}{2(1-\rho)^2(4x-4x^2-\rho)^2} g_{z\alpha} - \frac{\rho[-4x(2-9x+6x^2)+\rho(1-10x+2\rho)]}{2(1-\rho)^2(4x-4x^2-\rho)^2} \\ \quad - \frac{\rho[(2+\rho)g_{z\alpha}+3)]}{4(1-\rho)^{5/2}} \ln\frac{2x-1+\sqrt{1-\rho}}{2x-1-\sqrt{1-\rho}} & x<0 \end{cases}, \tag{45}$$

$$\tilde{f}_p(x,\rho) = \frac{\alpha_s C_F}{2\pi}\begin{cases} \frac{-4x\rho(3-5x+2x^2)+\rho^2(4-3x+4x^2-4x^3)-\rho^3}{(1-x)(1-\rho)^2(4x-4x^2-\rho)} g_{z\alpha} + \frac{-2x\rho(5-6x)+\rho^2(3-2x)}{(1-\rho)^2(4x-4x^2-\rho)} \\ \quad + \left[\frac{-2\rho(1-4x+2x^2)-\rho^2(2-x+2x^2)+\rho^3}{2(1-x)(1-\rho)^{5/2}} g_{z\alpha} + \frac{-\rho(2-6x+\rho)}{2(1-\rho)^{5/2}}\right] \ln\frac{2x-1+\sqrt{1-\rho}}{2x-1-\sqrt{1-\rho}} & x>1 \\ \frac{\rho(1-2x)(4-3x-\rho)}{(1-x)(1-\rho)^2} g_{z\alpha} + \frac{-2x+3\rho-4x\rho}{(1-\rho)^2} \\ \quad + \left[\frac{-\rho(2-8x+4x^2)-\rho^2(2-x+2x^2)+\rho^3}{2(1-x)(1-\rho)^{5/2}} g_{z\alpha} + \frac{-\rho(2-6x+\rho)}{2(1-\rho)^{5/2}}\right] \ln\frac{1+\sqrt{1-\rho}}{1-\sqrt{1-\rho}} & 0<x<1 \\ -\frac{-4x\rho(3-5x+2x^2)+\rho^2(4-3x+4x^2-4x^3)-\rho^3}{(1-x)(1-\rho)^2(4x-4x^2-\rho)} g_{z\alpha} - \frac{-2x\rho(5-6x)+\rho^2(3-2x)}{(1-\rho)^2(4x-4x^2-\rho)} \\ \quad - \left[\frac{-2\rho(1-4x+2x^2)-\rho^2(2-x+2x^2)+\rho^3}{2(1-x)(1-\rho)^{5/2}} g_{z\alpha} + \frac{-\rho(2-6x+\rho)}{2(1-\rho)^{5/2}}\right] \ln\frac{2x-1+\sqrt{1-\rho}}{2x-1-\sqrt{1-\rho}} & x<0 \end{cases}$$
$$+ \frac{\alpha_s C_F}{2\pi}(1-\tau)\begin{cases} \frac{16x\rho(1-3x+2x^2)+4x^2\rho^2(3-2x)-\rho^3(5-2x)+2\rho^4}{2(1-\rho)^2(4x-4x^2-\rho)^2} g_{z\alpha} \\ \quad + \frac{\rho(1-2x)[16x(1-x)-2\rho(1+2x-2x^2)-\rho^2]}{2(1-\rho)^2(4x-4x^2-\rho)^2} + \frac{-\rho(4-\rho)(g_{z\alpha}+1)}{4(1-\rho)^{5/2}} \ln\frac{2x-1+\sqrt{1-\rho}}{2x-1-\sqrt{1-\rho}} & x>1 \\ \frac{\rho(5-2\rho)g_{z\alpha}+2+\rho}{2(1-\rho)^2} + \frac{-\rho(4-\rho)(g_{z\alpha}+1)}{4(1-\rho)^{5/2}} \ln\frac{1+\sqrt{1-\rho}}{1-\sqrt{1-\rho}} & 0<x<1 \\ -\frac{16x\rho(1-3x+2x^2)+4x^2\rho^2(3-2x)-\rho^3(5-2x)+2\rho^4}{2(1-\rho)^2(4x-4x^2-\rho)^2} g_{z\alpha} \\ \quad - \frac{\rho(1-2x)[16x(1-x)-2\rho(1+2x-2x^2)-\rho^2]}{2(1-\rho)^2(4x-4x^2-\rho)^2} - \frac{-\rho(4-\rho)(g_{z\alpha}+1)}{4(1-\rho)^{5/2}} \ln\frac{2x-1+\sqrt{1-\rho}}{2x-1-\sqrt{1-\rho}} & x<0 \end{cases}. \tag{46}$$

ξ^2 be small but not vanishing

Apply OPE to non-local op $\mathcal{O}_n(\xi)$

$$\sigma_n(\omega, \xi^2, P^2) = \sum_{J=0} \sum_a W_n^{(J,a)}(\xi^2, \mu^2)\, \xi^{\nu_1} \cdots \xi^{\nu_J} \times \langle P | \mathcal{O}^{(J,a)}_{\nu_1 \cdots \nu_J}(\mu^2) | P \rangle \,,$$

$\mathcal{O}^{(J,a)}_{\nu_1 \cdots \nu_J}(\mu^2)$ Local, symmetric , traceless op

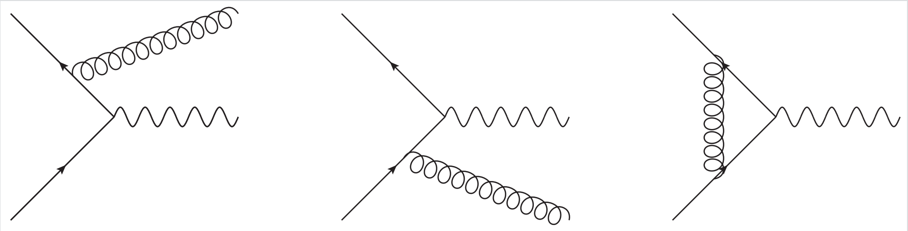

Figure 3.1.: NLO Feynman diagrams contributing to the Drell-Yan cross section.

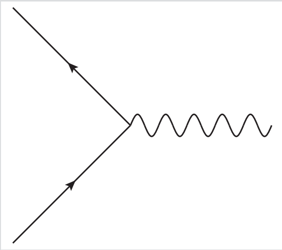

Figure 5.1.: LO Feynman diagram contributing to the Drell-Yan process.

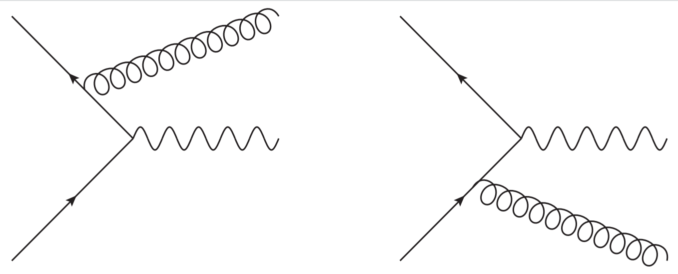

Figure 5.2.: Real gluon-emission diagrams for the Drell-Yan process at NLO.

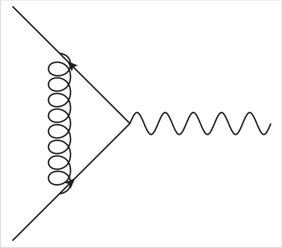

Figure 5.3.: Virtual diagram contributing to the Drell-Yan cross section at NLO.